Offline analysis of the chemical composition and hygroscopicity of sub-micrometer aerosol at an Asian outflow receptor site and comparison with online measurements

Yange Deng[1,2,3], Hiroaki Fujinari[1], Hikari Yai[1], Kojiro Shimada[4,5], Yuzo Miyazaki[6], Eri Tachibana[6], Dhananjay K. Deshmukh[7], Kimitaka Kawamura[7], Tomoki Nakayama[2,8], Shiori Tatsuta[4], Mingfu Cai[9,10], Hanbing Xu[9], Fei Li[11,12], Haobo Tan[11], Sho Ohata[13,14,15], Yutaka Kondo[16], Akinori Takami[17], Shiro Hatakeyama[4,18], and Michihiro Mochida[1,2]

[1] Graduate School of Environmental Studies, Nagoya University, Nagoya, 464-8601, Japan
[2] Institute for Space-Earth Environmental Research, Nagoya University, Nagoya, 464-8601, Japan
[3] Now at National Institute for Environmental Studies, Tsukuba, 305-8506, Japan
[4] Faculty of Agriculture, Tokyo University of Agriculture and Technology, Tokyo, 183-8538, Japan
[5] Now at Department of Chemistry, Biology, and Marine Science, University of the Ryukyus, Okinawa, 903-0213, Japan
[6] Institute of Low Temperature Science, Hokkaido University, Sapporo, 060-0819, Japan
[7] Chubu Institute for Advanced Studies, Chubu University, Kasugai, Aichi, 487-8501, Japan
[8] Now at Graduate School of Fisheries and Environmental Sciences, Nagasaki University, Nagasaki, 852-8521, Japan
[9] School of Atmospheric Sciences, Sun Yat-sen University, Zhuhai, Guangdong, 519082, China
[10] Now at Institute for Environmental and Climate Research, Jinan University, Guangzhou, Guangdong, 511443, China
[11] Institute of Tropical and Marine Meteorology, China Meteorological Administration, Guangzhou, 510-640, China
[12] Now at Xiamen Key Laboratory of Straits Meteorology, Xiamen Meteorological Bureau, Xiamen, 361012, China
[13] Department of Earth and Planetary Science, The University of Tokyo, Tokyo, 113-8654, Japan
[14] Now at Institute for Space-Earth Environmental Research, Nagoya University, Nagoya, 464-8601, Japan
[15] Now at Institute for Advanced Research, Nagoya University, Nagoya, 464-8601, Japan
[16] National Institute of Polar Research, Tokyo, 190-8518, Japan
[17] National Institute for Environmental Studies, Tsukuba, 305-8506, Japan
[18] Now at Asia Center for Air Pollution, Japan Environmental Sanitation Center, Niigata, 950-2144, Japan

Correspondence to: Michihiro Mochida (mochida@isee nagoya-u ac jp)

Abstract. Filter-based offline analysis of atmospheric aerosol hygroscopicity coupled to composition analysis provides information complementary to that obtained from online analysis However, its application itself and comparison to online analysis have remained limited to date In this study, daily submicrometer aerosol particles ($PM_{0.95}$, 50 % cutoff diameter: 0 95 μm) were collected onto quartz fiber filters in Okinawa Island, a receptor of East Asian outflow, in the autumn of 2015 The chemical composition of water-soluble matter (WSM) in $PM_{0.95}$ and $PM_{0.95}$ itself, and their respective hygroscopicities were characterized through the offline use of an aerosol mass spectrometer and a hygroscopicity tandem differential mobility analyzer Thereafter, results were compared with those obtained from online analyses Sulfate dominated the WSM mass (59 %), followed by water-soluble organic matter (WSOM, 20 %) and ammonium (13 %) WSOM accounted for most (91 %) of the mass of extracted organic matter (EOM) and the atomic O to C ratios (O:C) of WSOM and EOM were high (mean ±

削除: 60

削除: 93

standard deviation were, respectively, 0 84±0 08 and 0 78±0 08), both of which indicate highly aged characteristics of the observed aerosol The hygroscopic growth curves showed clear hysteresis for most samples At 85 % RH, the calculated hygroscopicity parameter κ of the WSM (κ_{WSM}), WSOM, EOM, and $PM_{0.95}$ ($\kappa_{PM0.95}$) were, respectively, 0 50±0 03, 0 22±0 12, 0 20±0 11, and 0 47±0 03 An analysis using the thermodynamic E-AIM model shows, on average, that inorganic salts and WSOM respectively contributed 88 % and 12 % of the κ_{WSM} (or $\kappa_{PM0.95}$) High similarities were found between offline and online analysis for chemical compositions that are related to particle hygroscopicity (the mass fractions and O:C of organics, and the degree of neutralization), and also for aerosol hygroscopicity As possible factors governing the variation of κ_{WSM}, the influences of WSOM abundance and the neutralization of inorganic salts were assessed At high RH (70–90 %), the hygroscopicity of WSM and $PM_{0.95}$ was affected considerably by the presence of organic components; at low RH (20–50 %), the degree of neutralization could be important This study not only characterized aerosol hygroscopicity at the receptor site of East Asian outflow, but also shows that the offline hygroscopicity analysis is an appropriate method, at least for aerosols of the studied type The results encourage further applications to other environments and to more in-depth hygroscopicity analysis, in particular for organic fractions

削除: 79

1 Introduction

Hygroscopicity of atmospheric aerosols is a key property related to its effects on climate and air quality It influences the aerosol's light scattering and absorption ability (Titos et al , 2016; Zhou et al , 2020) and therefore affects visibility and the radiative balance of the Earth Moreover, it influences the capability of aerosol particles to act as cloud condensation nuclei (CCN) under supersaturated water-vapor conditions, which further influences the radiative balance by affecting the optical property and lifetime of clouds (Mcfiggans et al , 2006) In addition, the absorption of water by aerosol particles might serve as important media for aqueous-phase reactions (McNeill, 2015; Cheng et al , 2016) The hygroscopicity of aerosol particles might also influence their adverse effects on human health: aerosol particle deposition in a human body is expected to depend on hygroscopic growth under high relative humidity (RH) in the respiratory system (Braakhuis et al , 2014)

The hygroscopicity of atmospheric aerosol is governed by the chemical composition It is often represented by hygroscopicity parameter κ Several hygroscopicity studies have been performed for atmospheric particles or particles generated by extracts from atmospheric aerosol samples Whereas the ability of the particles to grow to cloud droplet size under supersaturated water vapor conditions has been investigated using a cloud condensation nucleus (CCN) counter, alternatively, the growth of particle size as a result of humidification under sub-saturated conditions has also been investigated, for example using a hygroscopicity tandem differential mobility analyzer (HTDMA) At water activity (a_w) of around 0 9 or higher, inorganic salts such as NaCl and $(NH_4)_2SO_4$ present high κ values of 0 5–1 4; atmospheric organic aerosol (OA) components present intermediate κ values of 0 01–0 5 (Petters and Kreidenweis, 2007) By contrast, black carbon retains almost no water (Guo et al , 2016) and its κ value can be inferred as zero The κ values of ambient aerosol particles are explained by the combination of water uptake by

respective components in the mixture In the low to middle RH range, the deliquescence and efflorescence of inorganic salts can strongly affect the hygroscopic growth of atmospheric particles, and could result in hysteresis according to the history of RH (Tang et al , 1977) For the hygroscopicity of ambient particles, the composition of inorganics, including the degree of neutralization, affects their contribution to particle hygroscopicity (Tang and Munkelwitz, 1977; Freedman et al , 2019) In addition, the contrasting hygroscopicity of organics and inorganics are responsible for variations of their hygroscopicity (e g , Gunthe et al , 2009; Cerully et al , 2011; Pierce et al , 2012; Levin et al , 2014; Deng et al , 2018) The dominant components of atmospheric aerosols govern the dependence of aerosol hygroscopicity on locations: hygroscopicity in the forest atmosphere (Gunthe et al , 2009; Hong et al , 2014), where OA dominates the aerosol composition, is generally less than that in the marine atmosphere (Mochida et al , 2011; Pringle et al , 2010), where inorganic salts dominate Moreover, while the oxygenation of OA relates to its hygroscopicity (Kuwata et al , 2013), correlation from analysis of atmospheric aerosols can be poor (Kuang et al , 2020) Whereas multiple compositional factors are expected to control the aerosol hygroscopic growth as explained above, studies elucidating variations of hygroscopic growth under different atmospheric environments are few, which can be attributed to the lack of hygroscopicity analyses coupled with chemical composition analyses

For characterizing the hygroscopicity of atmospheric aerosols, offline analysis, i e , the collection of aerosol samples on substrates, followed by analysis of the hygroscopicity of chemical components therein, provides information that complements information obtained from online analysis Such offline analyses have been conducted for urban aerosols (e g , Aggarwal et al , 2007; Mihara and Mochida, 2011) and aerosols in remote environments (e g , Silvergren et al , 2014; Boreddy and Kawamura, 2016) For offline methods, hygroscopicity of aerosol particles with size up to ~1 μm or larger was analyzed, providing data for hygroscopicity in a wide range of particle sizes, which are often difficult to obtain by online analyses Furthermore, whereas information related to the mixing state is lost, offline methods enable investigation of the hygroscopicity of specific compound groups in aerosols, for example, water-soluble matter and humic-like substances (Gysel et al , 2004) Moreover, whereas field deployments of online instruments such as HTDMA might be a heavy duty and hinder observations particularly at remote sites, offline analysis can be a good alternative for aerosol hygroscopicity studies Recent studies have indicated that offline use of an aerosol mass spectrometer (AMS) can be a useful means to elucidate the contribution of OA component to aerosol hygroscopicity because of its capability of quantifying organic mass in addition to organic carbon, and to characterize the chemical structure of OA (Mihara and Mochida, 2011; Lee et al , 2019) More offline studies, in particular those of the role of OA, should be undertaken to characterize aerosol hygroscopicity further

Positive and negative artifacts have been evaluated for offline analyses of the concentrations of aerosol chemical components (Turpin et al , 2000; Chow et al , 2005) Sampling artifacts are inherent to offline analyses, and might also affect offline hygroscopic growth measurements However, the propriety of the offline method for quantifying aerosol hygroscopicity is not evaluated tentatively Bias might arise from sampling artifacts by adsorption or evaporative loss of compounds and degradation of collected aerosol components, as in the case of the quantification of chemical components Although full resolution of the

degree of such artifacts is difficult, comparison between offline and online results from measurements of chemical composition and aerosol hygroscopicity is expected to constrain the possible magnitudes of artifacts, and warrant the further utilization of offline methods

In this study, we analyzed the hygroscopicity of submicrometer ($PM_{0.95}$, 50 % cutoff diameter: 0 95 μm) aerosol samples collected in Okinawa, a remote island in Japan We interpreted results based on the chemical composition analysis, including the offline use of an aerosol mass spectrometer Okinawa is considered a receptor site of aerosols from the Asian continent, thereby suited to characterize the nature of the hygroscopicity of aged atmospheric aerosols after long-range transport Although a few reports have described the relation between the chemical composition and the hygroscopicity in Okinawa (Mochida et al , 2010; Cai et al , 2017), no report of the relevant literature has described a study of their mutual quantitative relation Here, based on measurements of the chemical composition of $PM_{0.95}$ and the hygroscopic growth of the extracted water-soluble matter (WSM) in $PM_{0.95}$, the hygroscopicity parameter κ of WSM, water-soluble organic matter (WSOM), and $PM_{0.95}$ at 20–90 % RH are characterized Factors responsible for the hygroscopicity parameters are assessed This study, an extension of our online aerosol hygroscopicity study (Cai et al , 2017), aims at characterizing the RH and composition dependence of the hygroscopicity of aged aerosols after their atmospheric transport In addition, from a methodological viewpoint, the offline analysis of the composition and hygroscopic growth using filter samples are assessed by comparison with online analysis

2 Experimental

2.1 Aerosol sampling and extraction

Aerosol samples were collected at Cape Hedo Atmosphere and Aerosol Monitoring Station (128 15 °E, 26 52 °N) of the National Institute for Environmental Studies, Japan, in Okinawa Island during 26 October and 9 November, 2015 It is a receptor site of Asian outflow after long-range transport (Takami et al , 2007; Lun et al , 2014) The aerosols were collected daily on quartz fiber filters using a high-volume aerosol sampler (Model-120 B; Kimoto Electric Co Ltd) equipped with a cascade impactor (TE-234; Tisch Environmental Inc) Details of sampling periods for the respective samples are presented in Table S1 The respective means of the RH, air temperature, and wind speed during the sampling days were 75 4 %, 23 8 °C, and 3 8 m s^{-1} Precipitation was only observed on 30 October (Fig S1) The $PM_{0.95}$ samples collected on backup filters (area: 391 cm^2) were used for analysis The quartz fiber filters were pre-combusted at 450 °C for 6 h before use The high-volume sampler was placed on the rooftop of a station building Its inlet was located about 4 m above the ground The flow rate of the sampler was about 1,100 L min^{-1} For each sample, about 1,600 m^3 of air was aspirated Blank samples were collected by operating the sampler for only 10 s After sample collection, the filter samples were stored in freezers for around nine months or longer before the analyses Possible degradation of some highly reactive compounds such as persistent radicals (Alpert et al , 2021) is not assessed in this study

削除: before analysis

For offline analyses using the HTDMA and the AMS, WSM and water-insoluble organic matter (WISOM) in each aerosol sample were extracted as follows First, three punches (34 mm diameter) from each filter sample were ultrasonicated with ~3 g water for 15 min The solution was then filtered with a Teflon filter (0 20 μm, Millex-FG; Millipore Corp) For each aerosol sample, the extraction was repeated three times and the WSM solutions were combined Then, the WISOM in the same sample punches were extracted by ultrasonication with first 3 g of methanol once and then 3 g of dichloromethane/methanol (2/1, v/v) mixture three times The extract solutions were filtered through the Teflon filter used for the filtration of WSM, and the solutions after filtration were combined The combined WISOM solution was dried with a rotatory evaporator and was re-dissolved in dichloromethane/methanol (2/1, v/v) solution For total organic carbon (TOC) analyses for WSM, three punches (diameter: 34 mm) of each filter sample were extracted ultrasonically once with 20 ml ultrapure water for 15 min before being filtered through a syringe filter; similarly, for ion chromatograph (IC) analyses for WSM, one punch with a diameter of 34 mm was extracted with 10 ml ultrapure water (20 min ultra-sonication) and then filtered (Müller et al , 2017b) The fair agreement between the mass concentrations of extracted OC from the offline AMS analysis, the performance of which has been well validated in the work of Chen et al (2016), and those of OC from the thermal analysis support the high extraction efficiency of organics by the solvent extraction

削除: IC

2.2 Hygroscopic growth measurement for WSM

The hygroscopic growth factors (g_f) of WSM at 20, 30, 40, 50, 60, 65, 70, 75, 80, 85, and 90% RH in humidification and dehumidification branches were obtained using an HTDMA (Fig S2a) For measurements, a WSM solution was nebulized using a home-made nebulizer equipped with a syringe pump to generate WSM aerosol particles After the generated WSM aerosol was passed through a Nafion humidifier (NH1, 94–98 % RH MH-110-12F-4; Perma Pure LLC), it was dried with two diffusion dryers in series containing silica gel (White, Middle Granule; Kanto Kagaku) and a molecular sieve (13X/4A mixture; Supelco and Sigma-Aldrich) The dried aerosol flow was transferred through an impactor (model 1035900; TSI Inc) with a 0 071 cm diameter orifice in the front It was then neutralized using an Am^{241} neutralizer The neutralized aerosol was passed through the first differential mobility analyzer (DMA1, Model 3081; TSI Inc) in the HTDMA The aerosol particles with 100 nm dry diameter were selected In humidification mode, dry 100 nm aerosol particles were then humidified using a second Nafion humidifier (NH2, MD-110-24S-4; Perma Pure LLC) In dehumidification mode, dry 100 nm particles were first humidified to > 97 % RH using a third Nafion humidifier (NH3, MD-110-24S-4; Perma Pure LLC) before the particles were transferred to NH2

削除:

The aerosol particles downstream of NH2 were scanned using a second DMA (DMA2, Model 3081; TSI Inc) coupled with a condensation particle counter (CPC, model 3775; TSI Inc) The aerosol flow rates of both DMA1 and DMA2 were 0 3 L min^{-1} The RH values at the outlet of sheath flow of the DMA1, the inlet of NH2, the inlets of sample and sheath flows of the DMA2, and the outlet of sheath flow of the DMA2 were monitored using RH sensors (HMT337; Vaisala) During the

experiment, the RH inside the DMA1 was lower than 10 % The residence time from the outlet of the NH2 to the inlet of DMA2 was calculated as 13 s, which is close to the lower end of the recommended range of 10–~40 s by Duplissy et al (2009) The g_f at 90 % RH in humidification and dehumidification branches was measured separately one month later than the g_f at other RH The g_f is defined as the ratio of the mobility diameter of particles classified using DMA2 to the dry mobility diameter (100 nm), which were retrieved using the Twomey algorithm with consideration of transfer functions of the two DMAs as the work in Mochida et al (2010) ("T" in Eq S2 in the reference should be omitted) but with modified data bins The mode g_f of fitted lognormal distributions under different RH conditions were used to represent the hygroscopic growth of WSM and for the derivation of the hygroscopicity parameter (κ_{WSM}) following the κ- Köhler theory (Petters and Kreidenweis, 2007) as

$$\kappa_{WSM} = (g_f^3 - 1)\left[\frac{\exp\left(\frac{4\sigma M_w}{RT\rho_w d_{wet}}\right)}{RH} - 1\right], \quad (1)$$

where σ represents the surface tension at the solution–air interface, M_w and ρ_w respectively denote the molecular mass and density of pure water, d_{wet} stands for the product of g_f and d_{dry} (here is 100 nm), R is the universal gas constant, and T is the absolute temperature In Eq (1), T of 298 15 K was used considering the temperature at the outlet of sheath flow of DMA2 (24 22–26 59 °C) The surface tension of pure water was σ The equations used to calculate the density and surface tension of pure water and the densities of dry inorganic salts are the same as those used in the online Extended AIM Aerosol Thermodynamics (E-AIM) model (Sect 2 5) Measurement data were used to derive g_f and κ_{WSM} only if the RH values at the outlet of DMA2 meet certain criteria (Text S1) Note that the assumption of 30 % lower σ than that of water (Facchini et al , 1999) results in a slight decrease in the calculated κ_{WSM} (0 8–3 4 %), which provides guide in the uncertainty associated with surface tension

Before hygroscopic growth measurements for aerosol extracts, the size selection performance of DMA1 and DMA2 was assessed using PSL particles of standard size (Text S2) Furthermore, the hygroscopic growth of pure ammonium sulfate (AS, 99 999 % trace metals basis; Aldrich) particles were measured following the same procedure as that for the WSM samples to confirm the HTDMA performance (Text S3) The g_f of dry AS particles (RH = 7 22±0 04 %) was measured to quantify the slight difference of sizing (1 9 %) between the two DMAs This difference has been corrected for derivation of g_f of WSM samples and AS particles More details about the quality control of the offline analyses are presented in Text S4

2.3 Chemical composition analyses

Ammonium, nitrate, sulfate, sodium, potassium, calcium, magnesium, chloride, and methane sulfonic acid (MSA) in WSM samples were quantified using an ion chromatograph (Model 761 compact IC; Metrohm AG) Concentrations of water-soluble organic carbon (WSOC) in WSM samples were determined using a total organic carbon analyzer (Model TOC-L_{CHP}; Shimadzu Corp) The results are presented in Table S3

削除:

削除: as described by Mochida et al (2010)

To characterize the chemical structures of WSOM and WISOM and to quantify their concentrations, WSM and WISOM samples were analyzed using a high-resolution time-of-flight mass spectrometer (AMS; Aerodyne Research Inc ; Decarlo et al , 2006) by nebulizing the solutions using Ar and by transferring the generated particles to the AMS Before analysis by AMS, the WSM aerosol flow was dried using two diffusion driers filled with silica gel The WISOM aerosol flow was dried by two diffusion driers filled in series with activated carbon (to remove dichloromethane and methanol vapor) and silica gel The AMS were operated in both V-mode and W-mode The W-mode data were analyzed to obtain the atomic ratios of O to C (O:C), H to C (H:C), and organic mass to organic carbon (OM:OC) based on the Improved-Ambient method (Canagaratna et al , 2015) for WSOM and WISOM The O:C and H:C of WSOM and WISOM were used further to derive their densities (Kuwata et al , 2012) The mass concentration of WSOM was calculated as the product of WSOC from the TOC analyzer and the OM:OC of WSOM To validate the quantification of WSOM and derive the mass ratios of WISOM to WSOM, the mass spectra of WSOM and WISOM, and those of the mixtures of phthalic acid and WSOM (or WISOM) from V-mode AMS analysis were used for their quantification (Text S5) The mass concentration of WISOM was calculated as the product of the mass concentration of WSOM and the mass ratio of WISOM to WSOM from the mass spectral analysis The mass concentration of extracted organic matter (EOM) was defined as the sum of WSOM and WISOM The mass concentration of water-insoluble organic carbon (WISOC) was derived by dividing the mass concentration of WISOM by the OM:OC of WISOM The extracted organic carbon (EOC) was defined as the sum of WSOC and WISOC

The concentrations of OC and elemental carbon (EC) in $PM_{0.95}$ aerosol samples were obtained using a Sunset Laboratory carbon analyzer with the Interagency Monitoring of Protected Visual Environments (IMPROVE_A) temperature protocol and the thermal-optical transmission method A filter punch of 16 mm diameter was used for the analysis, and the presence of carbonate carbon was not considered Good agreement (Fig S6) was found between EOC and OC, indicating high recovery of EOM Table S4 summaries all offline measurements

削除: found

削除: S5

2.4 Concurrent online measurements of ambient aerosol

削除: ¶

During the period of the filter sampling of $PM_{0.95}$, the mass concentrations of non-refractory chemical components (sulfate, nitrate, ammonium, chloride, and organics) and black carbon (BC) in PM_1 (50 % cutoff diameter: 1 μm) were measured respectively using the same AMS as that for the offline analysis, and a filter-based absorption photometer continuous soot monitoring system (COSMOS; Kanomax, Osaka, Japan) (Mori et al , 2014; Ohata et al , 2019) Furthermore, the number–size distributions of submicrometer aerosols were measured using a scanning mobility particle sizer (SMPS) composed of a DMA (model 3081; TSI Inc) and a water-based CPC (model 3785; TSI Inc) A schematic of the experimental setup for AMS/SMPS measurements is presented in Fig S2b The AMS was operated in both V + pToF-mode and W-mode with time resolution of 30 min The bulk mass concentrations of non-refractory aerosol components were derived from V-mode data Composition-dependent collection efficiency (Middlebrook et al , 2012) was applied for quantification The W-mode data were analyzed to

obtain the O:C and H:C and densities of organics in the manner of the offline analysis The SMPS measured the aerosol number-size distributions at diameters of 13 8–749 9 nm every 5 min The DMA in the SMPS was operated with an aerosol flow rate of 0 3 LPM and a sheath to aerosol flow ratio of 10:1 Compressed dry pure air was supplied to the CPC through an equalizer to complement its total inlet flow rate of 1 0 LPM Temperature and RH of ambient air, wind speed and direction, and precipitation were measured using a weather sensor (model WXT520; Vaisala) The AMS was calibrated before both online and offline (Sect 2 3) measurements using the same procedures as those reported by Deng et al (2018) The SMPS was calibrated using standard size PSL particles (Text S2) before ambient measurements Furthermore, a hygroscopicity and volatility tandem differential mobility analyzer (H/V-TDMA) was deployed during 1–9 November 2015 to measure the size-resolved aerosol hygroscopicity and volatility Related details have been presented by Cai et al (2017) For comparison between offline and online data, the time windows for offline data were truncated to 10 am to 10 am (24 h) Online data were averaged for the one-day periods (Table S1)

2.5 Prediction of WSM hygroscopicity based on E-AIM model

Hygroscopic growth of the WSM sample for the water activity (a_w) range of 0 10–0 99 was predicted without considering the water uptake by WSOM using the online Extended AIM Aerosol Thermodynamics Model III (E-AIM III, http://www aim env uea ac uk/aim/model3/model3a php, last access: 1 August 2019; Clegg et al , 1998; Wexler and Clegg, 2002) The inorganic chemical components of WSM (sulfate, sodium, and ammonium) obtained from IC analysis and the WSOM obtained from TOC and offline AMS analyses were used for derivation Potassium, calcium, magnesium, nitrate, and chloride were not considered in the E-AIM because of their very low concentrations (Table S3) The RH-dependent hygroscopicity parameters of WSM, κ_{WSM}, were predicted from hygroscopic growth data following the κ- Köhler theory The RH-dependent hygroscopicity parameters of water-soluble inorganic matter (WSIM) in each WSM sample, κ_{inorg}, were derived similarly to those for κ_{WSM} Details of these derivations are presented in Text S6

2.6 Estimating the hygroscopicity of WSOM, EOM, and $PM_{0.95}$

The hygroscopicity parameters of WSOM (κ_{WSOM}), EOM (κ_{EOM}), and $PM_{0.95}$ ($\kappa_{PM0.95}$) were calculated on the assumption that the volumes of water retained by respective components are additive (Petters and Kreidenweis, 2007):

$$\kappa_{WSM} = \varepsilon_{WSOM/WSM}\kappa_{WSOM} + \varepsilon_{WSIM/WSM}\kappa_{inorg} \quad (2)$$

Therein, κ_{WSM} is the hygroscopicity parameter of WSM particles; κ_{WSOM} and κ_{inorg} respectively denote hygroscopicity parameters of WSOM and WSIM The $\varepsilon_{WSOM/WSM}$ and $\varepsilon_{WSIM/WSM}$ respectively stand for the volume fractions of WSOM and WSIM in WSM, as derived from offline IC, TOC, and AMS analyses (Text S7)

The hygroscopicity parameter of EOM was estimated on the assumption that the hygroscopicity parameter of WISOM, κ_{WISOM}, is zero, as

$$\kappa_{EOM} = \varepsilon_{WSOM/EOM}\kappa_{WSOM} + \varepsilon_{WISOM/EOM}\kappa_{WISOM} = \varepsilon_{WSOM/EOM}\kappa_{WSOM}, \quad (3)$$

where $\varepsilon_{WSOM/EOM}$ and $\varepsilon_{WISOM/EOM}$ respectively represent the volume fractions of WSOM and WISOM in EOM (Text S7) With consideration of EC and WISOM but neglecting other water-insoluble inorganics in $PM_{0.95}$, the hygroscopicity parameter of $PM_{0.95}$ was also estimated

$$\kappa_{PM0.95} = \varepsilon_{WSM/PM0.95}\kappa_{WSM} + \varepsilon_{WISOM/PM0.95}\kappa_{WISOM} + \varepsilon_{EC/PM0.95}\kappa_{EC}$$

$$= \varepsilon_{WSM/PM0.95}\kappa_{WSM} \quad (4)$$

Therein, $\varepsilon_{WSM/PM0.95}$, $\varepsilon_{WISOM/PM0.95}$, and $\varepsilon_{EC/PM0.95}$ respectively represent the volume fractions of WSM, WISOM, and EC among the sum of these three components (Text S7) Here, the hygroscopicity of EC, κ_{EC}, was assumed to be zero

3 Results and Discussion

3.1 Mass concentrations and composition of aerosol components

The atmospheric mass concentrations of chemical components in $PM_{0.95}$ samples and their mass fractions are presented in Fig 1 along with the mass concentrations of chemical components and number-size distributions of aerosols from online analyses Offline analysis of $PM_{0.95}$ samples indicated that sulfate was most abundant (mean ± standard deviation: 2 62±1 70 μg m^{-3}) throughout the observation period, followed by WSOM (0 86±0 51 μg m^{-3}), ammonium (0 59±0 32 μg m^{-3}), WISOM (0 11±0 14 μg m^{-3}), EC (0 10±0 03 μg m^{-3}), and sodium (0 07±0 03 μg m^{-3}) Accordingly, sulfate accounted for the largest mass fraction (59 4 %) among the quantified $PM_{0.95}$ components, followed by WSOM (19 6 %), ammonium (13 3 %), WISOM (2 56 %), EC (2 36 %), and sodium (1 49 %) The contributions of potassium, magnesium, calcium, nitrate, and chloride to the $PM_{0.95}$ samples were small: 1 23 % in total WSOM accounted for a major fraction of EOM (mean of 91 % on a mass basis) This large proportion suggests that the studied aerosol was aged substantially, considering the much lower proportions against total OM in East Asian suburban (approx 60 %; Müller et al , 2017a) and urban environments (27–45 %; Miyazaki et al , 2006), which are based on our mass conversions, assuming factors of 1 8 and 1 2 to convert WSOC to WSOM and WISOC to WISOM (Müller et al , 2017a and references therein), respectively The mass ratio of EC to EOM was on average 11 %, which is similar to the proportion to total OM (12 %) based on earlier reported OC:EC over the Sea of Japan and offshore of Japan (Lim et al , 2003; a factor of 2 1 (Turpin and Lim, 2001) was assumed to convert OC to OM) As shown in Fig 1d, the aerosol number–size distribution shows bimodal or broad unimodal characteristics

削除: EC (0 10±0 03 μg m^{-3}),
削除: 10
削除: 5
削除: 7
削除: 4
削除: WISOM (2 33 %),
削除: 50
削除: 93
削除: ,

For sulfate, organics, ammonium, and EC (BC), the relative abundances among them from the offline analysis showed moderate agreement with those from the online analysis (61 7 %, 22 2 %, 13 7 %, and 2 4 %, respectively, for sulfate, EOM, ammonium, and EC from offline measurements during the period with effective data) The coefficients of determination (r^2) of the mass fractions of sulfate, organics, ammonium, and EC (BC) in those four aerosol components from offline and online analyses were, respectively, 0 62, 0 32, 0 23, and 0 08 (Fig S7) Whereas the absolute concentrations of the aerosol are not crucially important for the offline analysis of aerosol hygroscopicity, high positive correlations between online and offline measurements for sulfate, organics, ammonium, and EC (BC) (r^2 of which are, respectively, 0 90, 0 82, 0 92, and 0 76; Fig S7) support agreement between offline and online analyses Note that the r^2 of the mass fractions between offline and online analyses were lower than those of the mass concentrations It may be in part because the mass fractions of respective components are influenced by the uncertainties of the mass concentrations of respective components and also by those of the summed concentrations In addition, smaller variations of the mass fractions as compared to the mass concentrations may result in larger contributions of the uncertainties to r^2 The average mass concentrations of sulfate, organics, and ammonium from online measurements were, respectively, 77 %, 76 %, and 71 % of offline results Lower concentrations might result from uncertainty of the collection efficiency of the online AMS analysis (Takegawa et al , 2009), and from different size windows for offline $PM_{0.95}$ sampling and online AMS analysis Sampling bias of organics or ammonium by absorption/evaporation does not explain the difference because sulfate measurements should not be influenced largely from positive/negative artifacts, considering its low volatility (Johnson et al , 2004) and reported absence of SO_2 artifacts for filters of other types (Eldred and Cahill, 1997) The mean mass concentration of BC from online analysis was almost equal to those of EC from the offline analysis: the ratio of the former to the latter was 1 02

Figure 2 presents backward air mass trajectories for $PM_{0.95}$ sampling For most days, the three-day trajectories passed over the Asian continent and/or the Japan archipelago, but maritime air masses also arrived at the observation site during 6–8 November 2015 A comparison between air mass trajectories and aerosol concentration data shows that maritime air masses during 6–8 November are characterized by lower aerosol mass concentrations, but higher mass fractions of sodium (≥5 %) than the other days influenced by continental air masses (Figs 1a, 1b and 2) The mean mass concentrations of sulfate, WSOM, ammonium, and EC from offline analyses during 6–8 November were, on average, 1/6, 1/5, 1/5, and 1/2 of those during other days, respectively, whereas the mean mass concentration of sodium during the period (0 07 μg m^{-3}) was similar to that of other days (0 06 μg m^{-3}) (Table S3)

Two types of composition related to aerosol hygroscopicity were investigated: the O:C of organics and the molar ratio of ammonium to sulfate (after omitting sulfate that was preferentially neutralized by sodium) ($R_{A/S}$; Text S7), which represents the degree of neutralization of sulfate by ammonium and sodium For the derivation of $R_{A/S}$, the neutralization of sulfate by other cations was not considered because their contributions were small The O:C of EOM from $PM_{0.95}$ samples is presented in Figure 3a The mean ± standard deviation of the ratio was 0 78±0 08 Although the value was 18 % lower than that of the

削除: 9
削除: 0
削除: 8
削除: 31
削除: 22
削除: 09
削除: S6
削除: 83, 0 92, and 0 76; Fig S6) support agreement between offline and online analyses
削除: 77
削除:
削除: 79
削除: 16

mean O:C of OA from the online analysis of PM_1 (0 95±0 09), they were in good agreement (r^2=0 58; Fig S8) The O:C values of EOM were in the range of 0 64–0 94, suggesting a highly aged nature of the observed OA (Canagaratna et al , 2015) The $R_{A/S}$ values from $PM_{0.95}$ samples are presented in Fig 3b: the mean ± standard deviation was 1 45±0 34 The results suggest that except for the aerosols on 7 and 8 November, the studied aerosols were fairly acidic To compare the offline and online analyses, $R_{A/S}$ was also derived by ignoring the neutralization of sulfate by sodium, which is presented as $R_{A/S}'$ (Fig 3b) The mean ± standard deviation of $R_{A/S}'$ from the offline analysis (1 29±0 21) was similar to that from the online analysis (1 29±0 40) The two also showed good agreement (r^2=0 52; Fig S8) If a portion of sulfate was in the form of sodium sulfate at the time of online AMS analysis, then this fraction might have not been detected considering the high melting temperature of the salt However, the offline analysis suggests that the fraction of sulfate neutralized by sodium was, on average, only 5 % Hence, it is not expected to affect the comparison strongly Further comparisons between offline and online analyses based on mass spectra of organics are presented in Text S8

On 7 and 8 November, the days under the influence of maritime air masses, the O:C and $R_{A/S}$ from the offline analysis values were, respectively, lower and higher than those during other periods when the air masses were from the Asian continent and/or the Japan archipelago (Figs 2 and 3) In addition, comparison between $R_{A/S}'$ and $R_{A/S}$ from the offline analysis shows that sodium neutralized a larger fraction of sulfate on the two days The results suggest that air masses from the Asian continent transported more aged and acidic aerosol, and that air masses from the North Pacific included less-oxygenated and more-neutralized aerosol However, it is noteworthy that the possible influence of the external mixing state on the neutralization of aerosols is not considered The more-acidic nature of the continental aerosol is expected to be contributed by the formation of sulfate during the transport In addition, the oxidation of MSA from marine biological activity is expected to contribute to sulfate The low relative abundance of sodium in the continental aerosol also accounted for the more-acidic nature

3.2 Hygroscopicity of WSM and $PM_{0.95}$

The mean ± standard deviation of the measured g_f values for WSM particles are presented in Fig 4 and Table S5 The mean g_f values predicted from the E-AIM model without consideration of the water retained by WSOM are also shown in the figure The g_f values of the respective WSM samples are presented in Fig S11 While g_f smaller than unity was reported and interpreted as a result of restructuring of non-spherical particles (Gysel et al , 2004, Jung et al , 2011), the g_f of nearly unity or greater for WSM particles in our study (>0 997) means that such phenomenon was not evident It may owe to the humidification using NH1 followed by drying in diffusion driers prior to the HTDMA analysis, which may avoid fast water evaporation and formation of cracks or cavities (Gysel et al , 2004) The mean ± standard deviation of g_f at 40, 60 and 85 % RH in the humidification (dehumidification) branch were, respectively, 1 04±0 02 (1 09±0 03), 1 13±0 05 (1 22±0 01) and 1 53±0 03 (1 53±0 02) (Table S5) The obtained g_f of WSM at 90 % RH (g_f(90%)) was slightly lower than that of the WSM from Chichijima Island (1 76–1 79), which was also influenced by transport from East Asia but was much farther to the east of the Asian continent compared with Okinawa (Boreddy et al , 2014; Boreddy and Kawamura, 2016) It was also lower than

削除: S7
削除: S7
削除: ¶
削除: S4
削除: S8
削除: S4

the mean values for WSM during a cruise over the East China Sea (1 99, Yan et al , 2017), which was nearer the Asian continent On the other hand, the obtained g_f(90%) of WSM was higher than that of the WSM obtained during a cruise over the Bay of Bengal (1 25–1 43, Boreddy et al , 2016), which was influenced by anthropogenic or biomass burning air masses For three studies (Boreddy et al , 2014; Boreddy and Kawamura, 2016; Yan et al , 2017), the WSM were extracted from total suspended particles that contain higher mass fractions of inorganics and sea salts than those examined for this study By contrast, the WSM in the last referred study (Boreddy et al , 2016) was extracted from $PM_{2.5}$ (50 % cutoff diameter: 2 5 μm) with higher mass fractions of organics These compositional differences should explain the observed differences of g_f(90%)

Hysteresis of the hygroscopic growth of the WSM particles was observed for most samples except for those collected on 26 October and 2 and 6 November (Fig S11) The hysteresis was expected to have been caused by the influence of inorganic salts, as indicated by the differences in the predicted hygroscopic growth in humidification and dehumidification branches from the E-AIM model, where only the water retained by inorganics is considered Being different from the observation, the hysteresis was predicted for almost all samples, which might result from the uncertainty in the quantification of inorganic salts and/or the influence of organic components on the hygroscopicity of WSM (Choi and Chan, 2002) The deliquescence of WSM in the humidification branch was observed in the RH of 50–70 % In this branch, the WSM shows prominent water uptake at RH as low as 20 % (Fig 4a), being in contrast to the absence of hygroscopic growth of pure AS (Fig S3) Water uptake of WSM at low RH in the humidification branch can be enhanced under highly acidic conditions (Sect 3 1) and/or in the presence of WSOM (Gysel et al , 2004) In the dehumidification branch, efflorescence was not evident down to 30 % RH for most samples, indicating the existence of metastable conditions to retain water after experiencing high RH The samples collected on 7 and 8 November, all characterized by a large sodium fraction, showed clearer efflorescence behavior at 40 % RH (Fig S11) The high efflorescence RH (ERH) of sodium sulfate (57–59 %) (Tang, 1996) might have been associated with the observed efflorescence In addition, the high $R_{A/S}$ (2 01 and 1 97 respectively) on these two days could have contributed to the high ERH, which is supported by the distinctive ERH among different forms of ammoniated sulfate (Tang and Munkelwitz, 1994) Whereas the external mixing state of atmospheric aerosol is lost by filter sampling, the former possibility implies that the sea-salt component enhances the ability to effloresce once mixed with other inorganic components This characteristic, however, is expected to be important only if such aerosols are transported to drier environments

The obtained g_f values as a function of RH were converted to corresponding κ values The mean ± standard deviation of the measured κ values for WSM as a function of RH are presented in Fig 4b and Table S5 The κ values from the E-AIM by ignoring the water uptake by organics are also shown in the same figure The κ_{WSM} of respective WSM samples are presented in Fig S12 In the humidification branch, the measured κ_{WSM} averaged for each RH were 0 17–0 24 (at 20–50 % RH) and 0 50–0 56 (at 70–90 % RH), respectively below and above the marked increase in κ_{WSM} with the increase in RH, presumably indicating the deliquescence of major inorganic salts Comparison between measured κ_{WSM} versus predicted κ_{WSM} shows that,

削除: S8

削除: S2

削除: by

削除: 2014

削除: S8

削除: S4

削除: S9

on average, the measured κ_{WSM} were greater than predictions for all RH, suggesting the ubiquitous contributions of WSOM to the measured κ_{WSM} The results at RH < 70 % were more deviated from the 1:1 line than those at RH ≥ 70 % RH (Fig S13), which might indicate dominant contributions of WSOM to κ_{WSM} at low RH for some aerosol samples (Gysel et al , 2004; Aggawarl et al , 2007)

In the dehumidification branch, except for the case at 20 % RH, where the corresponding κ value was 0 17, the κ values of WSM were modestly high, with values of 0 42–0 57 The lack of a large dependence on RH suggests that efflorescence did not occur Even if it did, it was for minor fractions of inorganics The contribution of WSOM to the hygroscopicity of WSM was evident from the fact that, except the sample collected on 1 November, the E-AIM model predicted κ by ignoring the water retained by WSOM at RH ≥ 65 % were lower than the measured values (Fig S12) The κ values of WSM from respective $PM_{0.95}$ samples in dehumidification branches are presented in Fig 4c At high RH (≥ 65 %), the difference in κ_{WSM} among different samples was small compared with that at low RH, indicating that the difference in the composition among aerosol samples did not result in large variation in the hygroscopicity of WSM at these RH conditions Clear variations in hygroscopicity among samples at low RH can be explained by the influence of the degree of neutralization of inorganic salts and the abundance of organics For example, the κ_{WSM} on 1 November at ≤ 60 % RH was higher than on other days, which was likely to be related to a low $R_{A/S}$ ratio (approx 0 80), as evidenced by the large E-AIM predicted κ_{WSM} on this day (Fig S12); the κ_{WSM} on 26 October was lower than that on other days, which might be explained by the high mass fraction of WSOM (Fig 1b) in addition to the high $R_{A/S}$ (1 66) The contribution of chemical composition will be discussed further in later sections

By considering the atmospheric concentrations of WISOM and EC, the κ values of $PM_{0.95}$ were estimated (Table S5) In the humidification branch, the $\kappa_{PM0.95}$ were 0 16–0 22 and 0 47–0 53, respectively, without (20–50 % RH) and with (70–90 % RH) the deliquescence of WSM particles (Table S5) In the dehumidification branch, except for the case at 20 % RH, where the corresponding $\kappa_{PM0.95}$ was 0 16, they were in the range of 0 40–0 54 (Table S5) At 90 % RH, $\kappa_{PM0.95}$ was in the range of 0 47–0 52, which is higher than that measured at a supersite in Hong Kong (0 18–0 48 with d_{dry} of 100 and 200 nm, Cheung et al , 2015) that was influenced by clean maritime air masses and/or polluted Asian continental and coastal inflows

Figure 5 presents a comparison of calculated $\kappa_{PM0.95}$ at 85 % RH with that for 40–200 nm particles from the online analysis (κ_{online}) at 85 % RH during the same observation period The time series of the mean g_r of particles with different dry diameters are presented in Fig S14 The estimated range of $\kappa_{PM0.95}$ at 85 % RH (0 49–0 51) was within the range of κ_{online} (0 44–0 51) for ambient aerosol particles Furthermore, the $\kappa_{PM0.95}$ and κ_{online} at 85 % RH for 200 nm particles are compared for the days when both data are available (Fig 6) Moderate positive correlations were found (r^2 of 0 37 and 0 42 respectively for dehumidification and humidification branches), although the particle hygroscopicity stayed high and the variation was small during the campaign In addition, all data are within ~15 % from the 1:1 line (Fig 6) The absence of strong correlations may

削除: S10

削除: S9

削除: S9

削除: S4

削除: 15

削除: S4

削除: S4

削除: The estimated range of $\kappa_{PM0.95}$ at 85 % RH (0 49±0 02) was within the range of κ_{online} (0 44–0 51) for ambient aerosol particles

be because the offline/online data were for different size ranges, and because online data only represent less than 2 % of the aerosols in a day whereas offline data represent more than 95 % of aerosols in a day. Results obtained from comparison of $\kappa_{PM0.95}$ and κ_{online} indicate that offline aerosol hygroscopicity analysis can be used as an alternative method, at least for the studied type of aerosols, for which the sampling bias for semi-volatile ammonium nitrate is not significant because of its low abundance.

The mean number/volume concentrations as a function of dry particle diameter are also depicted in Fig. 5. The clear bimodal shape of the mean aerosol number–size distribution with Aitken and accumulation modes suggests that the aerosols experienced in-cloud processing (Mochida et al., 2011; Hoppel et al., 1986). Similar high hygroscopicity of particles in the Aitken mode (40 nm diameter) and the accumulation mode (150 and 200 nm diameters) suggests the dominance of sulfate in both modes (Mochida et al., 2011). The mean aerosol volume–number concentration presented unimodal distribution with mode diameter of 260 nm, indicating that aerosol mass in the accumulation mode dominates the total aerosol mass in the submicrometer size range. With regard to the influence of aerosol hygroscopicity on aqueous-phase chemical reactions on mass basis, the hygroscopicity of large aerosol particles in the accumulation mode might be more important. Offline analysis extended the online hygroscopic analysis of <200 nm particles to the whole submicrometer size range, where most of the aerosol liquid water mass should exist. Most HTDMA are not applicable to the measurements of the hygroscopicity of dry particles larger than 500 nm (Tang et al., 2019), although techniques to measure >500 nm particles have also been developed, for example based on the usage of optical particle counters (Sorooshian et al., 2008; Tang et al., 2019). Comparison with the κ of ambient particles with d_{dry} of 300 nm or larger in previous studies shows that the mean of κ at 85 % RH for $PM_{0.95}$ from our study (0.47) is larger than the mean κ values of 300–360 nm particles in an urban site (0.32–0.33; Kawana et al., 2016) and a forest site (0.34–0.40; Kawana et al., 2017; Deng et al., 2019) in East Asia.

削除: exists. The $\kappa_{PM0.95}$ and κ_{online} at 85 % RH for 200 nm particles are compared for the days when both data are available (Fig. 6), which showed moderate positive correlations: r^2 of 0.15 and 0.31 respectively for dehumidification and humidification branches. Results obtained from comparison of $\kappa_{PM0.95}$ and κ_{online} indicate that offline aerosol hygroscopicity analysis can be used as an alternative method, at least for the studied type of aerosols, for which the sampling bias for semi-volatile ammonium nitrate is not significant because of its low abundance.

3.3 Hygroscopicity of WSOM and EOM

The hygroscopicity parameters of WSOM and EOM were calculated based on κ_{WSM} from measurements in the dehumidification branch and the predicted water uptake by inorganic salts (Eqs. 2 and 3). The results are presented in Fig. 7 and Table S5. At 75–85 % RH, where the deviation of the measured κ of AS from that predicted from the E-AIM model was slight (≤ 5 %; Fig. S3), κ_{WSOM} values were 0.19–0.22. Those values were higher than the κ of WSOM from US national parks and Storm Peak Laboratory (0.05–0.15 at RH = 90 %; Taylor et al., 2017) and from fresh Indonesian peat burning particles (0.18 at RH = 85 %; Chen et al., 2017). In the same RH range, κ_{EOM} was in the range of 0.17–0.20, and was, on average, 11 % lower than that of κ_{WSOM}. The κ_{EOM} from this study was higher than the κ of OA in the Western/Central Los Angeles Basin that was influenced by marine air masses (0.14 at RH = 74–92 %; Hersey et al., 2011). It was also higher than the κ of OA that were influenced by marine air masses over the continental United States, Canada, the Pacific Ocean, and the Gulf of Mexico and were aged (O:C = 0.93 ± 0.30) (0.13 at RH = 70–95 %; Shingler et al., 2016). However, it might be lower than the κ of

削除: S4

削除: S2

削除: 9

OA at a supersite in Hong Kong, for which only an upper limit value of 0 29 (at 90 % RH) was reported (Yeung et al , 2014) It is noteworthy that the estimated mean κ_{WSOM} and κ_{EOM} of approx 0 2 is higher than the default κ value of organics (κ_{org}) of 0 14 used in an atmospheric aerosol model (Kawecki and Steiner, 2018) The different κ_{org} values of different types or different atmospheric regions reported in this study and earlier studies described above suggest the importance on considering different κ_{org} values depending on the types and origins of OA in model calculations The κ_{WSOM} and κ_{EOM} values derived from the measurement in the humidification branch at 85 % RH where WSM particles would be mostly or fully dissolved in water were also presented in Table S5 The mean values in the humidification branch were slightly higher than those in the dehumidification branch, but the characteristics explained above also apply to this condition The fractional contributions of WSOM to the water uptake by WSM and $PM_{0.95}$, represented respectively as $(\varepsilon_{WSOM/WSM} \times \kappa_{WSOM})/\kappa_{WSM}$ and $(\varepsilon_{WSOM/PM0.95} \times \kappa_{WSOM})/\kappa_{PM0.95}$, are presented in Table S6 The contribution of WSOM to the water uptake by WSM and $PM_{0.95}$ was 10–12 % at 75–85 % RH

The high κ_{WSOM} and κ_{EOM} values are reasonably explained by the high O:C ratios of WSOM and EOM on a mean basis The mean O:C of WSOM and EOM were 0 84 and 0 78, from which κ_{WSOM} and κ_{EOM} were estimated respectively to be 0 19 and 0 18 based on the reported regression lines between κ_{org} and O:C under sub-saturated and supersaturated conditions (0 42 ± 0 04 % supersaturation (Chang et al , 2010); 0 1–1 5 % supersaturation (Lambe et al , 2011); 90 % RH (Wu et al , 2013); 0 11–0 80 % supersaturation (Deng et al , 2018)) (Fig 7) Although there may be some difference in the κ_{org} between sub-saturated and supersaturated conditions, we regard our comparison is meaningful because the difference could be small (Liu et al , 2018 Kuang et al , 2020) Correlations of κ_{WSOM} and κ_{EOM} with the O:C were weak (Fig S15, dehumidification branch) That weakness, however, should not contradict earlier reported positive correlation between κ_{org} and O:C, given the narrow range of O:C observed in this study (0 64–0 94) The absence of correlation might also be related to the fact that the O:C values of WSOM and EOM fall in the plateau in the high O:C range reported by Cappa et al (2011), who reported sigmoidal dependence of the hygroscopicity of OA on the O:C

3.4 Factors affecting the hygroscopicity of WSM and $PM_{0.95}$

The discussion presented in earlier sections indicates that the water uptake of WSOM and the degree of neutralization of the inorganic components influence the hygroscopicity of WSM Here, the influences of the mass fraction of WSOM (f_{WSOM}) and $R_{A/S}$ on κ_{WSM} and $\kappa_{PM0.95}$ at 20–90 % RH are assessed in light of the variations of the hygroscopicity Although the variations of κ_{WSM} and $\kappa_{PM0.95}$ may also be contributed by other factors (e g , presence of minor inorganic ions, possible variation of κ_{WSOM}, and non-additivity of the contributions of WSOM and WSIM to the water uptake), they are not assessed here

The relation between f_{WSOM} and κ_{WSM} at 20–90 % RH in the dehumidification branch is presented in Figs 8a and 8b Despite the narrow range of f_{WSOM}, moderate negative correlation between f_{WSOM} and κ_{WSM} was observed for all RH conditions, except

削除: in
削除: to consider
削除: S4
削除: S5
削除: 79
削除: as
削除: ;
削除: ;
削除: ;
削除:)
削除: 7)
削除: S11
削除: ¶
削除: the mass fraction of WSOM (
削除:)

for 90 % RH, indicating the importance of the relative contributions of WSOM and WSIM (mainly sulfate + ammonium) to the hygroscopicity of WSM The poor correlation between f_{WSOM} and κ_{WSM} at 90 % RH in the dehumidification branch was probably attributable to measurement uncertainty, which is supported by the high correlation between f_{WSOM} and κ_{WSM} in the humidification branch (Fig 8b) This dependence is explained by the low hygroscopicity of WSOM compared to that of WSIM The shaded areas in Fig 8b represent κ_{WSM} predicted by application of mean (i e , fixed) value of κ_{inorg} and mean ± standard deviation of κ_{WSOM} for 85 % using Eq (2) The prediction captures the measured dependence of κ_{WSM} on f_{WSOM} at 85 % RH, supporting the importance of f_{WSOM} As in the case of κ_{WSM}, dependence of $\kappa_{PM0.95}$ on the mass fraction of EOM in $PM_{0.95}$ (f_{EOM}) in the dehumidification branch was also observed for ≥60 % RH except for 90 % RH (Figs S16a and S16b) The result suggests that the mass fractions of organic components played an important role in the variation of the hygroscopicity of aerosol particles

The relation between the degree of neutralization represented by $R_{A/S}$ and κ_{WSM} at 20–90 % RH is also analyzed for the dehumidification branch (Figs 8c and 8d) Although the correlations between $R_{A/S}$ and κ_{WSM} were weak for ≥60 % RH, clearer negative correlations were observed for <60 % RH This result implies that the degree of neutralization is important to the variation of κ_{WSM} under low RH conditions The correlation was absent for κ_{WSM} predicted from E-AIM versus measured $R_{A/S}$ (r^2≤0 33 for RH≤80 %) Therefore, the relation might be associated with the efflorescence behavior of inorganic components Negative correlation at <60 % RH was observed (r^2: 0 58–0 77) even after excluding two samples with high relative abundances of sodium, which showed high ERH (Fig 4c) Therefore, the efflorescence of ammoniated sulfate itself might be related to $R_{A/S}$ An alternative explanation is that $R_{A/S}$ is related to water uptake by organics and/or their influence on the efflorescence of inorganic salts Although the small amount of aerosol water at <60 % RH might not strongly affect the particle optical property, it might have an important role in chemical reactions in the particles Therefore, the relation between inorganic composition and water uptake should be assessed further, in addition to the role of acidity itself in the reactions As in the case of κ_{WSM}, the relation between $R_{A/S}$ and $\kappa_{PM0.95}$ in the dehumidification branch was analyzed (Figs S16c and S16d) The result suggests that the degree of neutralization of inorganic aerosol components is also important in low RH conditions

In the humidification branch, moderately to highly negative correlations were found between κ_{WSM} and f_{WSOM} (and $\kappa_{PM0.95}$ and f_{EOM}) at ≥ 70 % RH (Figs S17 and S18), indicating the contribution of WSOM to the water uptake of WSM (or $PM_{0.95}$), being similar to the case of the dehumidification branch Moderate positive (or negative) correlations of κ_{WSM} or $\kappa_{PM0.95}$ with $R_{A/S}$ were observed at 60 and 65 % RH (or 30 % RH), but for other RH conditions, correlation was not evident (Figs S17 and S18) This result contrasts with the prediction of κ_{WSM} from the E-AIM model (for inorganic components), which instead show moderate to high negative correlations with $R_{A/S}$ ratio, in particular at 50–70 % RH (r^2≥0 80; Fig S19) The strong positive correlations between E-AIM predicted DRH and $R_{A/S}$ ratio were also found (Fig S20) They are expected to be responsible for negative correlation between model-based κ_{WSM} and $R_{A/S}$ The reason for the contrasting results between the measurements

削除: Comparison
削除: shows high correlation, as presented in
削除:
削除: S12a
削除: S12b
削除: deliquescence
削除: S12c
削除: S12d
削除: S13
削除: S14
削除: S13
削除: S14
削除: S15
削除: S16

and the model prediction remains unclear Further investigations on the influence of the degree of neutralization of inorganic salts on κ_{WSM} (or $\kappa_{PM0.95}$) in the humidification mode are required While the measurement uncertainty for DRH as seen for AS might be responsible for the discrepancy, the possible role of WSOM on DRH of inorganic salts should also be explored in future studies

削除: causal relations between

削除: and

4 Summary and Conclusions

The composition of aerosols and the RH-dependent hygroscopic growth of aerosol components under the influence of the outflow from the Asian continent, as well as the air masses over the Pacific, were characterized based on analyses of submicrometer aerosol samples collected on filters in autumn 2015 in Okinawa, Japan This offline analysis compensated for online analysis in terms of the quantification and characterization of water-soluble components and $PM_{0.95}$ (50 % cutoff diameter: 0 95 μm), and of the measurement of the hygroscopic growth as a function of relative humidity This study characterized the RH-dependent hygroscopicity of submicrometer aerosols and their chemical components, in particular organics, in the outflow region of East Asia Moreover, results from offline analyses were compared to those collected using online methods to assess the consistency of the results from the two different approaches

削除: Another important point is that

The analysis of $PM_{0.95}$ samples collected on filters showed the dominance of sulfate, which is quantitatively consistent with the chemical composition analysis based on online analysis using AMS and COSMOS Offline analysis showed high proportions of WSOM (91 %) in EOM and high O:C of WSOM and EOM (0 84±0 08 and 0 78±0 08, respectively), all of which indicate the aged nature of the studied aerosol and characterize long-range transported aerosols off the coast of East Asia The temporal variation of the ammonium-to-sulfate molar ratio, assuming that sulfate was neutralized preferentially by sodium ions ($R_{A/S}$), was obtained from the offline analysis The result demonstrates that air masses from the Asian continent transported more acidic and aged aerosols and that sodium played a role in neutralizing the sulfate from maritime air masses

削除: 93

削除: 79

The RH dependence of hygroscopic growth in humidification and dehumidification branches was inferred for water-soluble components from filter samples At 40, 60, and 85 % RH, the κ values for WSM (κ_{WSM}) in the humidification (dehumidification) branch were, respectively, 0 21±0 10 (0 45±0 17), 0 30±0 13 (0 57±0 04) and 0 51±0 04 (0 50±0 03) The κ values for $PM_{0.95}$ ($\kappa_{PM0.95}$) were also calculated At 75–85 % RH, the κ values of WSOM and EOM in the dehumidification branch were estimated respectively as 0 19–0 22 and 0 17–0 20 The WSOM was estimated to have contributed to 10–12 % of the water uptake of WSM and $PM_{0.95}$ The dependences of the κ_{WSM} (or $\kappa_{PM0.95}$) on the mass fractions of WSOM in WSM (or $PM_{0.95}$), and the $R_{A/S}$ (at ≤50 % RH) in the dehumidification mode were inferred from their negative correlations In the humidification mode, whereas the mass fractions of WSOM was suggested to be important for both κ_{WSM} and $\kappa_{PM0.95}$ at RH ≥ 70 %, the relation between κ_{WSM} (or $\kappa_{PM0.95}$) and $R_{A/S}$ in the low RH range was not evident despite of the apparent relation in the case of κ_{WSM} predicted from E-AIM The dependence of κ_{WSM} and $\kappa_{PM0.95}$ on the fractions of WSOM and $R_{A/S}$ suggests the

importance to understand the temporal variability of the aerosol hygroscopicity at the receptor region of East Asian outflow, which includes a long-term trend under the condition of the large decrease of Chinese SO_2 emissions in recent years (Zheng et al , 2018)

The hygroscopicity parameter values of $PM_{0.95}$ at 85 % RH from offline methods were close to earlier reported values from online hygroscopicity measurements performed during the field campaign Results obtained from this study extended the characterization of the studied aerosols by online analysis (≤200 nm), toward the mass/volume based mean diameter of the submicrometer aerosols On the other hand, the similarity of the hygroscopicity parameter values from offline and online methods suggest the propriety of the offline method on aerosol hygroscopicity analysis, at least for remote sites at which the aerosols are aged and semi-volatile ammonium nitrate is not abundant This finding encourages further studies of the hygroscopicity of aerosol components, particularly OA, the hygroscopicity of which is not yet characterized well Given that precise analysis of the hygroscopicity of OA is not easy based on online analyses, the offline approach is useful for better understanding of the relation between chemical structure, sources and hygroscopicity of WSOM and other organic components, because of the richness of information from the AMS spectra For example, the hygroscopicity of humic-like substances and other organic fractions and their contributions to total particulate matter are worth elucidating by the extension of the approach of this study

Abbreviations and symbols

a_w	water activity
$\varepsilon_{EC/PM0.95}$	volume fraction of EC in $PM_{0.95}$
$\varepsilon_{EOM/PM0.95}$	volume fraction of EOM in $PM_{0.95}$
$\varepsilon_{WISOM/EOM}$	volume fraction of WISOM in EOM
$\varepsilon_{WSIM/PM0.95}$	volume fraction of WSIM in $PM_{0.95}$
$\varepsilon_{WSIM/WSM}$	volume fraction of WSIM in WSM
$\varepsilon_{WSOM/EOM}$	volume fraction of WSOM in EOM
$\varepsilon_{WSOM/WSM}$	volume fraction of WSOM in WSM
ρ_w	density of pure water
σ	surface tension at the solution–air interface of a liquid particle
κ	hygroscopicity parameter
κ_{EC}	κ of EC, which is equal to zero
κ_{EOM}	κ of EOM
κ_{inorg}	κ of WSIM

κ_{online}	κ of ambient aerosol particles at 85 % RH obtained through on-site measurement
$\kappa_{PM0.95}$	κ of $PM_{0.95}$
κ_{WSM}	κ of WSM
κ_{WSOM}	κ of WSOM
AMS	(high-resolution time-of-flight) aerosol mass spectrometer
AS	ammonium sulfate
BC	black carbon
COSMOS	continuous soot monitoring system
CPC	condensation particle counter
d_{dry}	dry particle diameter, which is 100 nm for this study
DMA	differential mobility analyzer
DRH	deliquescence RH
d_{wet}	wet particle diameter: the product of g_f and d_{dry}
E-AIM	online Extended AIM Aerosol Thermodynamics model
EC	elemental carbon
EOC	extracted organic carbon
EOM	extracted organic matter
ERH	efflorescence RH
g_f	hygroscopic growth factor
H:C	atomic ratio of H to C
H/V-TDMA	hygroscopicity and volatility tandem differential mobility analyzer
HTDMA	hygroscopicity tandem differential mobility analyzer
IC	ion chromatograph
M_w	molar mass of pure water
O:C	atomic ratio of O to C
OA	organic aerosol
OC	organic carbon
OM:OC	mass ratio of organic matter to organic carbon in the organic aerosol component
$PM_{0.95}$	subset of aerosol particles with diameters <0 95 μm
PM_1	subset of aerosol particles with diameters <1 μm
R	universal gas constant
r^2	coefficient of determination between two variables
$R_{A/S}$	molar ratio of ammonium to the remaining sulfate after preferentially being neutralized by sodium

$R_{A/S}'$	molar ratio of ammonium to sulfate
RH	relative humidity
SMPS	scanning mobility particles sizer
T	absolute temperature
TOC	total organic carbon
WISOC	water-insoluble organic carbon
WISOM	water-insoluble organic matter
WSM	water-soluble matter
WSIM	water-soluble inorganic matter
WSOC	water-soluble organic carbon
WSOM	water-soluble organic matter

Data availability. All of the finally derived data supporting the findings of this study are available in the article or in its supporting information file

Author contributions. MM, HF, and YD designed the experiments with contributions from KS and SH HF, YD, YH, and MM performed them with contributions from KS, YM, ET, DD, TN, ST, HX, FL, and SO YD, MM, and HF analyzed the data with contributions from KS, YM, ET, DD, KK, TN, ST, MC, HT, SO, YK, AT, and SH YD and MM prepared the manuscript with contributions from HF, YM, DD, SO, and AT

Competing interests. Author Kimitaka Kawamura is a member of the editorial board of the journal

Acknowledgments. We thank the staff of the Cape Hedo Atmosphere and Aerosol Monitoring Station, National Institute for Environmental Studies, Japan, for the use of the study site We also thank Atsushi Matsuki for the use of the water-based CPC, Petr Vodička for expert discussions on the OC/EC data analysis and comments on the paper, Martin Irwin for the field BC observation, and Naga Oshima for the quality control of online BC data We also thank Zhou Ruichen and Shuhei Ogawa for the calculation of the resident time of sample aerosols after humidification in the HTDMA We acknowledge the NOAA Air Resources Laboratory (ARL) for providing the HYSPLIT transport and dispersion model This study was supported in part by JSPS KAKENHI Grant Numbers JP19H04253 and JP18K19852 and the Environment Research and Technology Development Fund (JPMEERF20202003) of the Environmental Restoration and Conservation Agency of Japan, and was in part performed under the joint research program of Institute for Space–Earth Environmental Research, Nagoya University YD thanks the current affiliation for supporting her to process data and write this paper

References

Aggarwal, S G , Mochida, M , Kitamori, Y , and Kawamura, K : Chemical closure study on hygroscopic properties of urban aerosol particles in Sapporo, Japan, Environmental Science & Technology, 41, 6920-6925, 10 1021/es063092m, 2007

Alpert, P A , Dou, J , Arroyo, P C , Schneider, F , Xto, J , Luo, B P , Peter, T , Huthwelker, T , Borca, C N , Henzler, K D , Schaefer, T , Herrmann, H , Raabe, J , Watts, B , Krieger, U K , and Ammann, M : Photolytic radical persistence due to anoxia in viscous aerosol particles, Nature Communications, 12, 10 1038/s41467-021-21913-x, 2021

Boreddy, S K R , Kawamura, K , and Jung, J S : Hygroscopic properties of particles nebulized from water extracts of aerosols collected at Chichijima Island in the western North Pacific: An outflow region of Asian dust, Journal of Geophysical Research–Atmospheres, 119, 167-178, 10 1002/2013jd020626, 2014

Boreddy, S K R , and Kawamura, K : Hygroscopic growth of water-soluble matter extracted from remote marine aerosols over the western North Pacific: Influence of pollutants transported from East Asia, Science of the Total Environment, 557, 285-295, 10 1016/j scitotenv 2016 03 096, 2016

Boreddy, S K R , Kawamura, K , Bikkina, S , and Sarin, M M : Hygroscopic growth of particles nebulized from water-soluble extracts of PM2 5 aerosols over the Bay of Bengal: Influence of heterogeneity in air masses and formation pathways, Science of the Total Environment, 544, 661-669, 10 1016/j scitotenv 2015 11 164, 2016

Braakhuis, H M , Park, M , Gosens, I , De Jong, W H , and Cassee, F R : Physicochemical characteristics of nanomaterials that affect pulmonary inflammation, Part Fibre Toxicol , 11, 25, 10 1186/1743-8977-11-18, 2014

Cai, M F , Tan, H B , Chan, C K , Mochida, M , Hatakeyama, S , Kondo, Y , Schurman, M I , Xu, H B , Li, F , Shimada, K , Li, L , Deng, Y G , Yai, H , Matsuki, A , Qin, Y M , and Zhao, J : Comparison of Aerosol Hygroscopcity, Volatility, and Chemical Composition between a Suburban Site in the Pearl River Delta Region and a Marine Site in Okinawa, Aerosol and Air Quality Research, 17, 3194-3208, 10 4209/aaqr 2017 01 0020, 2017

Canagaratna, M R , Jimenez, J L , Kroll, J H , Chen, Q , Kessler, S H , Massoli, P , Hildebrandt Ruiz, L , Fortner, E , Williams, L R , Wilson, K R , Surratt, J D , Donahue, N M , Jayne, J T , and Worsnop, D R : Elemental ratio measurements of organic compounds using aerosol mass spectrometry: characterization, improved calibration, and implications, Atmospheric Chemistry and Physics, 15, 253-272, 10 5194/acp-15-253-2015, 2015

Cappa, C D , Che, D L , Kessler, S H , Kroll, J H , and Wilson, K R : Variations in organic aerosol optical and hygroscopic properties upon heterogeneous OH oxidation, Journal of Geophysical Research-Atmospheres, 116, 10 1029/2011jd015918, 2011

Cerully, K M , Raatikainen, T , Lance, S , Tkacik, D , Tiitta, P , Petaja, T , Ehn, M , Kulmala, M , Worsnop, D R , Laaksonen, A , Smith, J N , and Nenes, A : Aerosol hygroscopicity and CCN activation kinetics in a boreal forest environment during the 2007 EUCAARI campaign, Atmospheric Chemistry and Physics, 11, 12369-12386, 10 5194/acp-11-12369-2011, 2011

Chang, R Y W , Slowik, J G , Shantz, N C , Vlasenko, A , Liggio, J , Sjostedt, S J , Leaitch, W R , and Abbatt, J P D : The hygroscopicity parameter (kappa) of ambient organic aerosol at a field site subject to biogenic and anthropogenic influences: relationship to degree of aerosol oxidation, Atmospheric Chemistry and Physics, 10, 5047-5064, 10 5194/acp-10-5047-2010, 2010

Chen, J , Budisulistiorini, S H , Itoh, M , Lee, W C , Miyakawa, T , Komazaki, Y , Yang, L D Q , and Kuwata, M : Water uptake by fresh Indonesian peat burning particles is limited by water-soluble organic matter, Atmospheric Chemistry and Physics, 17, 11591-11604, 10 5194/acp-17-11591-2017, 2017

Chen, Q C , Ikemori, F , Higo, H , Asakawa, D , and Mochida, M : Chemical Structural Characteristics of HULIS and Other Fractionated Organic Matter in Urban Aerosols: Results from Mass Spectral and FT-IR Analysis, Environmental Science & Technology, 50, 1721-1730, 10 1021/acs est 5b05277, 2016

削除: Boreddy, S K R , Haque, M M , and Kawamura, K : Long-term (2001-2012) trends of carbonaceous aerosols from a remote island in the western North Pacific: an outflow region of Asian pollutants, Atmospheric Chemistry and Physics, 18, 1291-1306, 10 5194/acp-18-1291-2018, 2018 ¶

Cheng, Y F , Zheng, G J , Wei, C , Mu, Q , Zheng, B , Wang, Z B , Gao, M , Zhang, Q , He, K B , Carmichael, G , Poschl, U , and Su, H : Reactive nitrogen chemistry in aerosol water as a source of sulfate during haze events in China, Sci Adv , 2, 11, 10 1126/sciadv 1601530, 2016

Cheung, H H Y , Yeung, M C , Li, Y J , Lee, B P , and Chan, C K : Relative Humidity- Dependent HTDMA Measurements of Ambient Aerosols at the HKUST Supersite in Hong Kong, China, Aerosol Science and Technology, 49, 643-654, 10 1080/02786826 2015 1058482, 2015

Choi, M Y , and Chan, C K : The effects of organic species on the hygroscopic behaviors of inorganic aerosols, Environmental Science & Technology, 36, 2422-2428, 10 1021/es0113293, 2002

Chow, J C , Watson, J G , Lowenthal, D H , and Magliano, K L : Loss of PM2 5 nitrate from filter samples in central California, Journal of the Air & Waste Management Association, 55, 1158-1168, 10 1080/10473289 2005 10464704, 2005

Clegg, S L , Brimblecombe, P , and Wexler, A S : Thermodynamic model of the system H+-NH4+-SO42--NO3--H2O at tropospheric temperatures, Journal of Physical Chemistry A, 102, 2137-2154, 10 1021/jp973042r, 1998

DeCarlo, P F , Kimmel, J R , Trimborn, A , Northway, M J , Jayne, J T , Aiken, A C , Gonin, M , Fuhrer, K , Horvath, T , Docherty, K S , Worsnop, D R , and Jimenez, J L : Field-deployable, high-resolution, time-of-flight aerosol mass spectrometer, Analytical Chemistry, 78, 8281-8289, 10 1021/ac061249n, 2006

Deng, Y G , Kagami, S , Ogawa, S , Kawana, K , Nakayama, T , Kubodera, R , Adachi, K , Hussein, T , Miyazaki, Y , and Mochida, M : Hygroscopicity of Organic Aerosols and Their Contributions to CCN Concentrations Over a Midlatitude Forest in Japan, Journal of Geophysical Research-Atmospheres, 123, 9703-9723, 10 1029/2017jd027292, 2018

Deng, Y G , Yai, H , Fujinari, H , Kawana, K , Nakayama, T , and Mochida, M : Diurnal variation and size dependence of the hygroscopicity of organic aerosol at a forest site in Wakayama, Japan: their relationship to CCN concentrations, Atmospheric Chemistry and Physics, 19, 5889-5903, 10 5194/acp-19-5889-2019, 2019

Draxler, R R , and Hess, G D : An overview of the HYSPLIT_4 modelling system for trajectories, dispersion and deposition, Aust Meteorol Mag , 47, 295-308, 1998

Duplissy, J , Gysel, M , Sjogren, S , Meyer, N , Good, N , Kammermann, L , Michaud, V , Weigel, R , dos Santos, S M , Gruening, C , Villani, P , Laj, P , Sellegri, K , Metzger, A , McFiggans, G B , Wehrle, G , Richter, R , Dommen, J , Ristovski, Z , Baltensperger, U , and Weingartner, E : Intercomparison study of six HTDMAs: results and recommendations, Atmospheric Measurement Techniques, 2, 363-378, 10 5194/amt-2-363-2009, 2009

Eldred, R A , and Cahill, T A : Sulfate sampling artifact from SO2 and alkaline soil, Environmental Science & Technology, 31, 1320-1324, 10 1021/es9605533, 1997

Facchini, M C , Mircea, M , Fuzzi, S , and Charlson, R J : Cloud albedo enhancement by surface-active organic solutes in growing droplets, Nature, 401, 257-259, 10 1038/45758, 1999

Freedman, M A , Ott, E J E , and Marak, K E : Role of pH in Aerosol Processes and Measurement Challenges, Journal of Physical Chemistry A, 123, 1275-1284, 10 1021/acs jpca 8b10676, 2019

Gunthe, S S , King, S M , Rose, D , Chen, Q , Roldin, P , Farmer, D K , Jimenez, J L , Artaxo, P , Andreae, M O , Martin, S T , and Poschl, U : Cloud condensation nuclei in pristine tropical rainforest air of Amazonia: size-resolved measurements and modeling of atmospheric aerosol composition and CCN activity, Atmospheric Chemistry and Physics, 9, 7551-7575, 10 5194/acp-9-7551-2009, 2009

Guo, S , Hu, M , Lin, Y , Gomez-Hernandez, M , Zamora, M L , Peng, J F , Collins, D R , and Zhang, R Y : OH-Initiated Oxidation of m-Xylene on Black Carbon Aging, Environmental Science & Technology, 50, 8605-8612, 10 1021/acs est 6b01272, 2016

Gysel, M , Weingartner, E , Nyeki, S , Paulsen, D , Baltensperger, U , Galambos, I , and Kiss, G : Hygroscopic properties of water-soluble matter and humic-like organics in atmospheric fine aerosol, Atmospheric Chemistry and Physics, 4, 35-50, 10 5194/acp-4-35-2004, 2004

Hersey, S P , Craven, J S , Schilling, K A , Metcalf, A R , Sorooshian, A , Chan, M N , Flagan, R C , and Seinfeld, J H : The Pasadena Aerosol Characterization Observatory (PACO): chemical and physical analysis of the Western Los Angeles basin aerosol, Atmospheric Chemistry and Physics, 11, 7417-7443, 10 5194/acp-11-7417-2011, 2011

Hong, J , Hakkinen, S A K , Paramonov, M , Aijala, M , Hakala, J , Nieminen, T , Mikkila, J , Prisle, N L , Kulmala, M , Riipinen, I , Bilde, M , Kerminen, V M , and Petaja, T : Hygroscopicity, CCN and volatility properties of submicron atmospheric aerosol in a boreal forest environment during the summer of 2010, Atmospheric Chemistry and Physics, 14, 4733-4748, 10 5194/acp-14-4733-2014, 2014

Hoppel, W A , Frick, G M , and Larson, R E : Effect of Nonprecipitating Clouds on the Aerosol Size Distribution in the Marine Boundary-Layer, Geophysical Research Letters, 13, 125-128, 10 1029/GL013i002p00125, 1986

Johnson, G R , Ristovski, Z , and Morawska, L : Method for measuring the hygroscopic behaviour of lower volatility fractions in an internally mixed aerosol, Journal of Aerosol Science, 35, 443-455, 10 1016/j jaerosci 2003 10 008, 2004

Jung, J S , Kim, Y J , Aggarwal, S G , and Kawamura, K : Hygroscopic property of water-soluble organic-enriched aerosols in Ulaanbaatar, Mongolia during the cold winter of 2007, Atmospheric Environment, 45, 2722-2729, 10 1016/j atmosenv 2011 02 055, 2011

Kawana, K , Nakayama, T , and Mochida, M : Hygroscopicity and CCN activity of atmospheric aerosol particles and their relation to organics: Characteristics of urban aerosols in Nagoya, Japan, Journal of Geophysical Research-Atmospheres, 121, 4100-4121, 10 1002/2015jd023213, 2016

Kawana, K , Nakayama, T , Kuba, N , and Mochida, M : Hygroscopicity and cloud condensation nucleus activity of forest aerosol particles during summer in Wakayama, Japan, Journal of Geophysical Research-Atmospheres, 122, 3042-3064, 10 1002/2016jd025660, 2017

Kawecki, S , and Steiner, A L : The Influence of Aerosol Hygroscopicity on Precipitation Intensity During a Mesoscale Convective Event, Journal of Geophysical Research-Atmospheres, 123, 424-442, 10 1002/2017jd026535, 2018

Koike, M , and Oshima, N : Mass concentration of BC (black carbon) measurement by COSMOS at the Cape Hedo in Japan, 1 00, Arctic Data archive System (ADS), Japan, https://ads nipr ac jp/dataset/A20180402-006, 2018

Kuang, Y , Xu, W Y , Tao, J C , Ma, N , Zhao, C S , and Shao, M : A Review on Laboratory Studies and Field Measurements of Atmospheric Organic Aerosol Hygroscopicity and Its Parameterization Based on Oxidation Levels, Current Pollution Reports, 6, 410-424, 10 1007/s40726-020-00164-2, 2020

Kuwata, M , Zorn, S R , and Martin, S T : Using Elemental Ratios to Predict the Density of Organic Material Composed of Carbon, Hydrogen, and Oxygen, Environmental Science & Technology, 46, 787-794, 10 1021/es202525q, 2012

Kuwata, M , Shao, W , Lebouteiller, R , and Martin, S T : Classifying organic materials by oxygen-to-carbon elemental ratio to predict the activation regime of Cloud Condensation Nuclei (CCN), Atmospheric Chemistry and Physics, 13, 5309-5324, 10 5194/acp-13-5309-2013, 2013

Lambe, A T , Onasch, T B , Massoli, P , Croasdale, D R , Wright, J P , Ahern, A T , Williams, L R , Worsnop, D R , Brune, W H , and Davidovits, P : Laboratory studies of the chemical composition and cloud condensation nuclei (CCN) activity of secondary organic aerosol (SOA) and oxidized primary organic aerosol (OPOA), Atmospheric Chemistry and Physics, 11, 8913-8928, 10 5194/acp-11-8913-2011, 2011

Lee, W C , Chen, J Budisulistiorini, S H Itoh, M Shiodera S and Kuwata M : Polarity-dependent chemical characteristics of water-soluble organic matter from laboratory-generated biomass-burning revealed by 1-octanol-water partitioning, Environmental Science & Technology, 53, 8047-8056, 10 1021/acs est 9b01691, 2019

Levin, E J T , Prenni, A J , Palm, B B , Day, D A , Campuzano-Jost, P , Winkler, P M , Kreidenweis, S M , DeMott, P J , Jimenez, J L , and Smith, J N : Size-resolved aerosol composition and its link to hygroscopicity at a forested site in Colorado, Atmospheric Chemistry and Physics, 14, 2657-2667, 10 5194/acp-14-2657-2014, 2014

Lim, H J , Turpin, B J , Russell, L M , and Bates, T S : Organic and elemental carbon measurements during ACE-Asia suggest a longer atmospheric lifetime for elemental carbon, Environmental Science & Technology, 37, 3055-3061, 10 1021/es020988s, 2003

Liu, P F , Song, M J , Zhao, T N , Gunthe, S S , Ham, S H , He, Y P , Qin, Y M , Gong, Z H , Amorim, J C , Bertram, A K , and Martin, S T : Resolving the mechanisms of hygroscopic growth and cloud condensation nuclei activity for organic particulate matter, Nature Communications, 9, 10 1038/s41467-018-06622-2, 2018

Lun, X X , Takami, A , Ma, W F , Shimono, A , and Hatakeyama, S : Long-range transport of organic aerosol to Cape Hedo, Japan, Particuology, 13, 35-41, 10 1016/j partic 2013 04 010, 2014

McFiggans, G , Artaxo, P , Baltensperger, U , Coe, H , Facchini, M C , Feingold, G , Fuzzi, S , Gysel, M , Laaksonen, A , Lohmann, U , Mentel, T F , Murphy, D M , O'Dowd, C D , Snider, J R , and Weingartner, E : The effect of physical and chemical aerosol properties on warm cloud droplet activation, Atmospheric Chemistry and Physics, 6, 2593-2649, 10 5194/acp-6-2593-2006, 2006

McNeill, V F : Aqueous Organic Chemistry in the Atmosphere: Sources and Chemical Processing of Organic Aerosols, Environmental Science & Technology, 49, 1237-1244, 10 1021/es5043707, 2015

Middlebrook, A M , Bahreini, R , Jimenez, J L , and Canagaratna, M R : Evaluation of Composition-Dependent Collection Efficiencies for the Aerodyne Aerosol Mass Spectrometer using Field Data, Aerosol Science and Technology, 46, 258-271, 10 1080/02786826 2011 620041, 2012

Mihara, T , and Mochida, M : Characterization of Solvent-Extractable Organics in Urban Aerosols Based on Mass Spectrum Analysis and Hygroscopic Growth Measurement, Environmental Science & Technology, 45, 9168-9174, 10 1021/es201271w, 2011

Miyazaki, Y , Kondo, Y , Takegawa, N , Komazaki, Y , Fukuda, M , Kawamura, K , Mochida, M , Okuzawa, K , and Weber, R J : Time-resolved measurements of water-soluble organic carbon in Tokyo, Journal of Geophysical Research-Atmospheres, 111, 10 1029/2006jd007125, 2006

Mochida, M , Nishita-Hara, C , Kitamori, Y , Aggarwal, S G , Kawamura, K , Miura, K , and Takami, A : Size-segregated measurements of cloud condensation nucleus activity and hygroscopic growth for aerosols at Cape Hedo, Japan, in spring 2008, Journal of Geophysical Research-Atmospheres, 115, 16, 10 1029/2009jd013216, 2010

Mochida, M , Nishita-Hara, C , Furutani, H , Miyazaki, Y , Jung, J Y , Kawamura, K , and Uematsu, M : Hygroscopicity and cloud condensation nucleus activity of marine aerosol particles over the western North Pacific, Journal of Geophysical Research-Atmospheres, 116, 16, 10 1029/2010jd014759, 2011

Mori, T , Kondo, Y , Ohata, S , Moteki, N , Matsui, H , Oshima, N , and Iwasaki, A : Wet deposition of black carbon at a remote site in the East China Sea, Journal of Geophysical Research-Atmospheres, 119, 10 1002/2014jd022103, 2014

Müller, A , Miyazaki, Y , Aggarwal, S G , Kitamori, Y , Boreddy, S K R , and Kawamura, K : Effects of chemical composition and mixing state on size-resolved hygroscopicity and cloud condensation nuclei activity of submicron aerosols at a suburban site in northern Japan in summer, Journal of Geophysical Research-Atmospheres, 122, 9301-9318, 10 1002/2017jd027286, 2017a

Müller, A , Miyazaki, Y , Tachibana, E , Kawamura, K , and Hiura, T : Evidence of a reduction in cloud condensation nuclei activity of water-soluble aerosols caused by biogenic emissions in a cool-temperate forest, Sci Rep, 7, 9, 10 1038/s41598-017-08112-9, 2017b

Ohata, S , Kondo, Y , Moteki, N , Mori, T , Yoshida, A , Sinha, P R , and Koike, M : Accuracy of black carbon measurements by a filter-based absorption photometer with a heated inlet, Aerosol Science and Technology, 53, 1079-1091, 10 1080/02786826 2019 1627283, 2019

Petters, M D , and Kreidenweis, S M : A single parameter representation of hygroscopic growth and cloud condensation nucleus activity, Atmospheric Chemistry and Physics, 7, 1961-1971, 10 5194/acp-7-1961-2007, 2007

Pierce, J R , Leaitch, W R , Liggio, J , Westervelt, D M , Wainwright, C D , Abbatt, J P D , Ahlm, L , Al-Basheer, W , Cziczo, D J , Hayden, K L , Lee, A K Y , Li, S M , Russell, L M , Sjostedt, S J , Strawbridge, K B , Travis, M , Vlasenko, A , Wentzell, J J B , Wiebe, H A , Wong, J P S , and Macdonald, A M : Nucleation and condensational growth to CCN sizes during a sustained pristine biogenic SOA event in a forested mountain valley, Atmospheric Chemistry and Physics, 12, 3147-3163, 10 5194/acp-12-3147-2012, 2012

Pringle, K J , Tost, H , Pozzer, A , Poschl, U , and Lelieveld, J : Global distribution of the effective aerosol hygroscopicity parameter for CCN activation, Atmospheric Chemistry and Physics, 10, 5241-5255, 10 5194/acp-10-5241-2010, 2010

Shingler, T , Crosbie, E , Ortega, A , Shiraiwa, M , Zuend, A , Beyersdorf, A , Ziemba, L , Anderson, B , Thornhill, L , Perring, A E , Schwarz, J P , Campazano-Jost, P , Day, D A , Jimenez, J L , Hair, J W , Mikoviny, T , Wisthaler, A , and Sorooshian, A : Airborne characterization of subsaturated aerosol hygroscopicity and dry refractive index from the surface to 6 5km during the SEAC(4)RS campaign, Journal of Geophysical Research-Atmospheres, 121, 4188-4210, 10 1002/2015jd024498, 2016

Silvergren, S , Wideqvist, U , Strom, J , Sjogren, S , and Svenningsson, B : Hygroscopic growth and cloud forming potential of Arctic aerosol based on observed chemical and physical characteristics (a 1 year study 2007-2008), Journal of Geophysical Research-Atmospheres, 119, 14080-14097, 10 1002/2014jd021657, 2014

Sorooshian, A , Hersey, S , Brechtel, F J , Corless, A , Flagan, R C , and Seinfeld, J H : Rapid, size-resolved aerosol hygroscopic growth measurements: Differential aerosol sizing and hygroscopicity spectrometer probe (DASH-SP), Aerosol Science and Technology, 42, 445-464, 10 1080/02786820802178506, 2008

Takami, A , Miyoshi, T , Shimono, A , Kaneyasu, N , Kato, S , Kajii, Y , and Hatakeyama, S : Transport of anthropogenic aerosols from Asia and subsequent chemical transformation, Journal of Geophysical Research-Atmospheres, 112, 10 1029/2006jd008120, 2007

Takegawa, N , Miyakawa, T , Watanabe, M , Kondo, Y , Miyazaki, Y , Han, S , Zhao, Y , van Pinxteren, D , Bruggemann, E , Gnauk, T , Herrmann, H , Xiao, R , Deng, Z , Hu, M , Zhu, T , and Zhang, Y : Performance of an Aerodyne Aerosol Mass Spectrometer (AMS) during Intensive Campaigns in China in the Summer of 2006, Aerosol Science and Technology, 43, 189-204, 10 1080/02786820802582251, 2009

Tang, I N: Chemical and size effects of hygroscopic aerosols on light scattering coefficients, Journal of Geophysical Research-Atmospheres, 101, 19245-19250, 10 1029/96JD03003, 1996

Tang, I N , and Munkelwitz, H R : Aerosol growth studies – III ammonium bisulfate aerosols in a moist atmosphere, Journal of Aerosol Science, 8, 321-330, 10 1016/0021-8502(77)90019-2, 1977

Tang, I N , Munkelwitz, H R , and Davis, J G : Aerosol growth studies—II Preparation and growth measurements of monodisperse salt aerosols, Journal of Aerosol Science, 8, 149-159, 10 1016/0021-8502(77)90002-7, 1977

Tang, I N , and Munkelwitz, H R : Water Activities, Densities, and Refractive-Indexes of Aqueous Sulfates and Sodium-Nitrate Droplets of Atmospheric Importance, Journal of Geophysical Research-Atmospheres, 99, 18801-18808, 10 1029/94jd01345, 1994

Tang, M J , Chan, C K , Li, Y J , Su, H , Ma, Q X , Wu, Z J , Zhang, G H , Wang, Z , Ge, M F , Hu, M , He, H , and Wang, X M : A review of experimental techniques for aerosol hygroscopicity studies, Atmospheric Chemistry and Physics, 19, 12631-12686, 10 5194/acp-19-12631-2019, 2019

Taylor, N F , Collins, D R , Lowenthal, D H , McCubbin, I B , Hallar, A G , Samburova, V , Zielinska, B , Kumar, N , and Mazzoleni, L R : Hygroscopic growth of water soluble organic carbon isolated from atmospheric aerosol collected at US national parks and Storm Peak Laboratory, Atmospheric Chemistry and Physics, 17, 2555-2571, 10 5194/acp-17-2555-2017, 2017

Titos, G , Cazorla, A , Zieger, P , Andrews, E , Lyamani, H , Granados-Munoz, M J , Olmo, F J , and Alados-Arboledas, L : Effect of hygroscopic growth on the aerosol light-scattering coefficient: A review of measurements, techniques and error sources, Atmospheric Environment, 141, 494-507, 10 1016/j atmosenv 2016 07 021, 2016

Turpin, B J , and Lim, H J : Species Contributions to PM2 5 Mass Concentrations: Revisiting Common Assumptions for Estimating Organic Mass, Aerosol Science and Technology, 35, 602-610, 10 1080/02786820119445, 2001

Turpin, B J , Saxena, P , and Andrews, E : Measuring and simulating particulate organics in the atmosphere: problems and prospects, Atmospheric Environment, 34, 2983-3013, 10 1016/s1352-2310(99)00501-4, 2000

Wexler, A S , and Clegg, S L : Atmospheric aerosol models for systems including the ions H+, NH4+, Na+, SO42-, NO3-,Cl-, Br-, and H2O, Journal of Geophysical Research-Atmospheres, 107, 14, 10 1029/2001jd000451, 2002

Wu, Z J , Poulain, L , Henning, S , Dieckmann, K , Birmili, W , Merkel, M , van Pinxteren, D , Spindler, G , Muller, K , Stratmann, F , Herrmann, H , and Wiedensohler, A : Relating particle hygroscopicity and CCN activity to chemical composition during the HCCT-2010 field campaign, Atmospheric Chemistry and Physics, 13, 7983-7996, 10 5194/acp-13-7983-2013, 2013

Yan, Y , Fu, P Q , Jing, B , Peng, C , Boreddy, S K R , Yang, F , Wei, L F , Sun, Y L , Wang, Z F , and Ge, M F : Hygroscopic behavior of water-soluble matter in marine aerosols over the East China Sea, Science of the Total Environment, 578, 307-316, 10 1016/j scitotenv 2016 10 149, 2017

Yeung, M C , Lee, B P , Li, Y J , and Chan, C K : Simultaneous HTDMA and HR-ToF-AMS measurements at the HKUST Supersite in Hong Kong in 2011, Journal of Geophysical Research-Atmospheres, 119, 9864-9883, 10 1002/2013jd021146, 2014

Zheng, B , Tong, D , Li, M , Liu, F , Hong, C P , Geng, G N , Li, H Y , Li, X , Peng, L Q , Qi, J , Yan, L , Zhang, Y X , Zhao, H Y , Zheng, Y X , He, K B , and Zhang, Q : Trends in China's anthropogenic emissions since 2010 as the consequence of clean air actions, Atmospheric Chemistry and Physics, 18, 14095-14111, 10 5194/acp-18-14095-2018, 2018

Zhou, J C , Xu, X Z , Zhao, W X , Fang, B , Liu, Q Q , Cai, Y Q , Zhang, W J , Venables, D S , and Chen, W D : Simultaneous measurements of the relative-humidity-dependent aerosol light extinction, scattering, absorption, and single-scattering albedo with a humidified cavity-enhanced albedometer, Atmospheric Measurement Techniques, 13, 2623-2634, 10 5194/amt-13-2623-2020, 2020

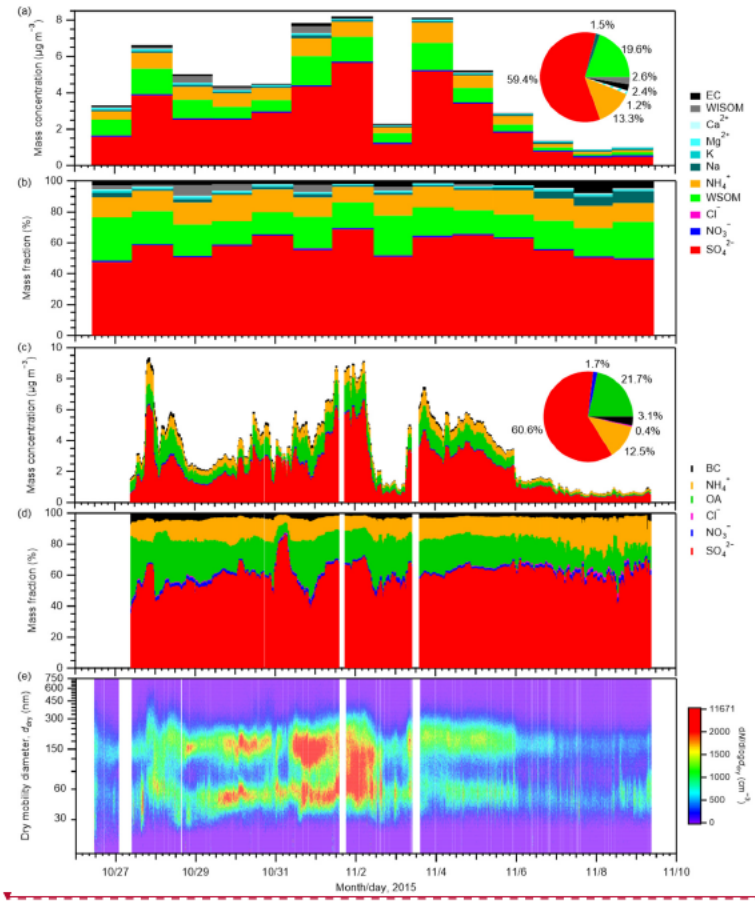

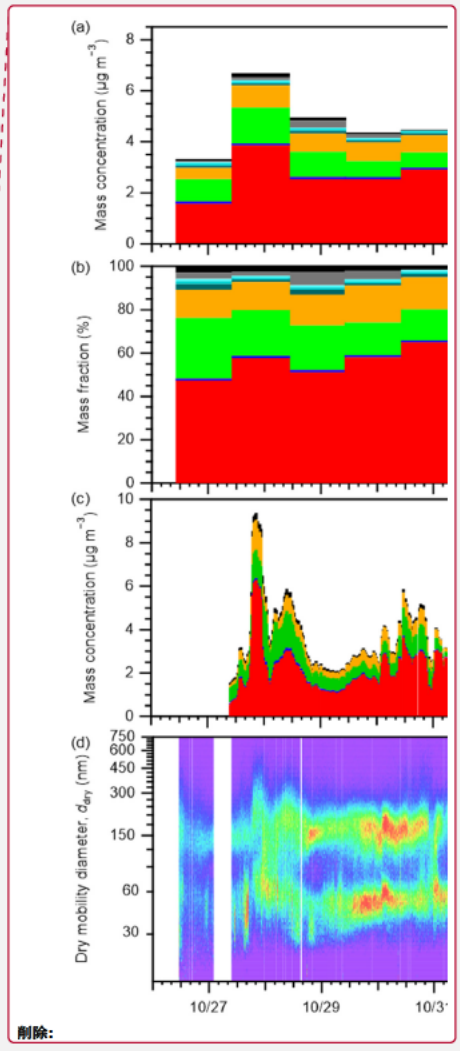

削除:

Figure 1: (a) Mass concentrations of chemical components in $PM_{0.95}$ and (b) their mass fractions from offline analyses. (c) Mass concentrations of PM_1 components and (d) their mass fractions, and (e) number–size distributions of aerosol particles from online analyses. A related online BC data has been published by Koike and Oshima (2018). The pie charts in panels (a) and (c) show the mean fractions of each compound calculated from their mean mass concentrations based on offline and online analyses, respectively. The pattern wedge in the pie chart in panel (a) represent the total mass fraction of K^+, Mg^{2+}, Ca^{2+}, Cl^-, and NO_3^-. The composition and size distribution of the aerosols at the study site are also discussed in Cai et al. (2017).

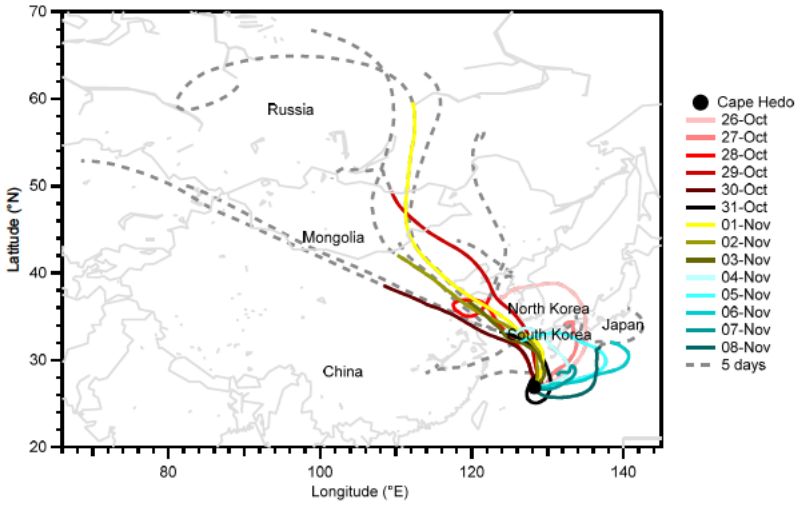

Figure 2: Daily air mass trajectories arrived at 500 m above the observation site at 1400 JST. The solid-colored lines represent the three-day trajectories. The solid-colored lines together with their respective extended gray dash sections indicate the five-day trajectories. The solid circle represents the observation site location. The map is based on GSHHG 2.3.4; the shoreline polygon data in crude resolution is used. Trajectories were produced using NOAA HYSPLIT atmospheric transport and dispersion modeling system (Draxler and Hess, 1998).

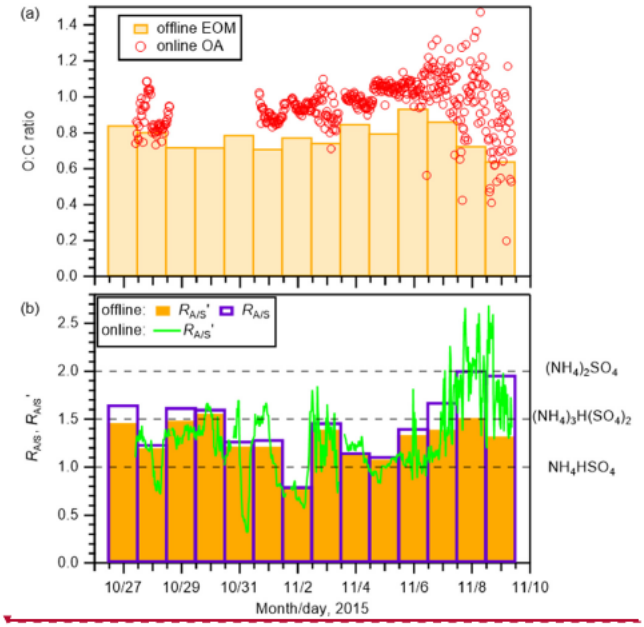

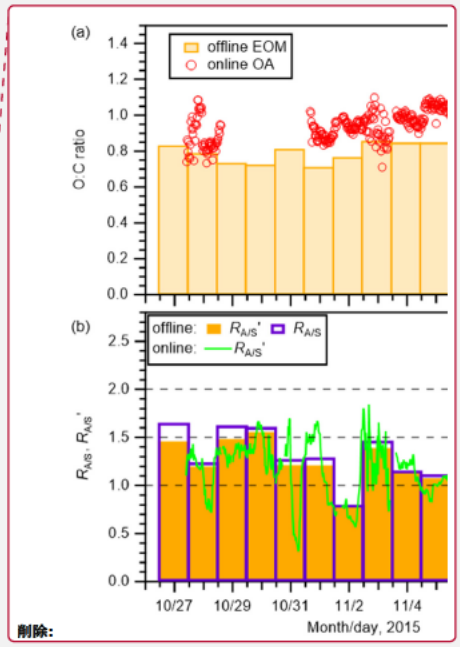

Figure 3: (a) The O:C of EOM from the offline analysis of $PM_{0.95}$ samples (bars) and that of OA from the online AMS analysis (open circles). (b) The degree of neutralization of the remaining sulfate (after preferentially being neutralized by sodium; Text S7) by ammonium from the offline analysis of $PM_{0.95}$ samples ($R_{A/S}$; box bars); the degree of neutralization of sulfate by ammonium (without considering sodium) ($R_{A/S}$') from the offline analysis (solid bars) and the online AMS analysis (solid line). The $R_{A/S}$' values of NH_4HSO_4, $(NH_4)_3H(SO_4)_2$, and $(NH_4)_2SO_4$ are shown as dashed lines in panel (b). In panel (a), the missing of O:C during 28–31 October is due to the malfunction of chopper in the W-mode online measurement.

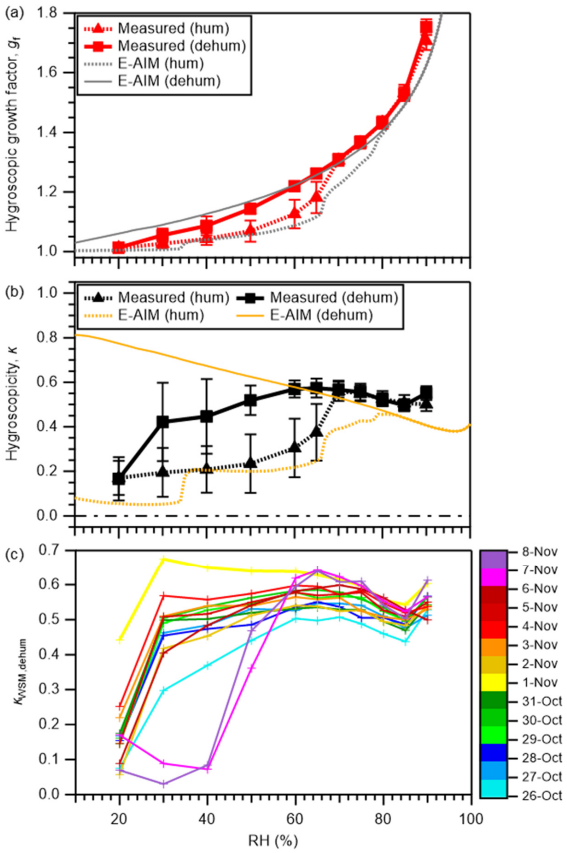

Figure 4: The mean of (a) measured and E-AIM predicted g_f for WSM particles as a function of RH and (b) measured and E-AIM predicted κ_{WSM} as a function of RH. (c) The κ values for WSM from respective $PM_{0.95}$ samples in dehumidification (dehum) branches. In panels (a) and (b), results from both humidification (hum) and dehumidification branches are presented. In the predictions in panels (a) and (b), water retained by WSOM are not considered. Results obtained for the dehumidification branch were obtained by assuming that no solid is formed under any RH condition.

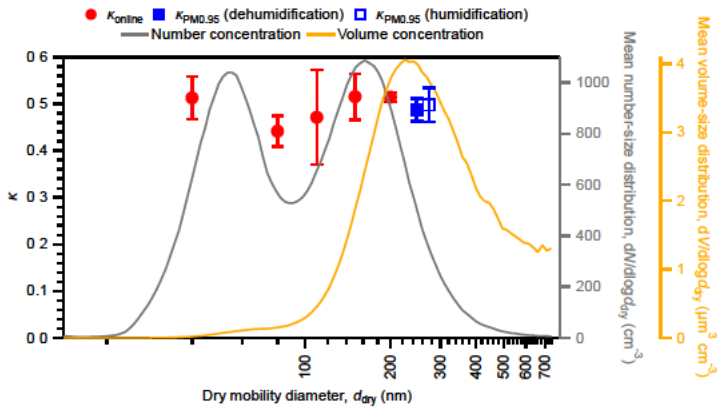

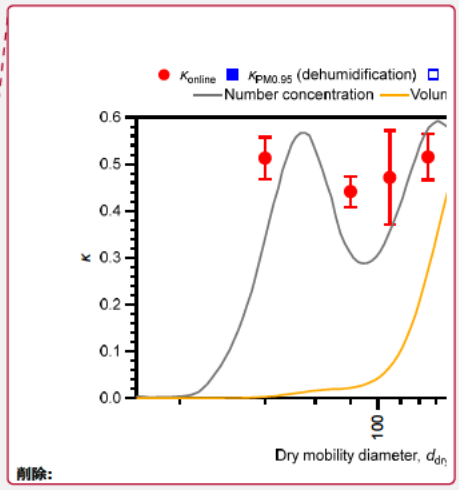

Figure 5: Comparison of κ at 85 % RH for PM0.95 (κPM0.95) in humidification and dehumidification branches, and that from online analyses (κonline) during the same observation period. Markers and whiskers respectively represent mean values and standard deviations. The mean number/volume size distributions of atmospheric aerosols are also shown. The size distribution and κonline of the aerosols at the study site are also discussed in Cai et al. (2017).

削除: κ

削除: concentrations

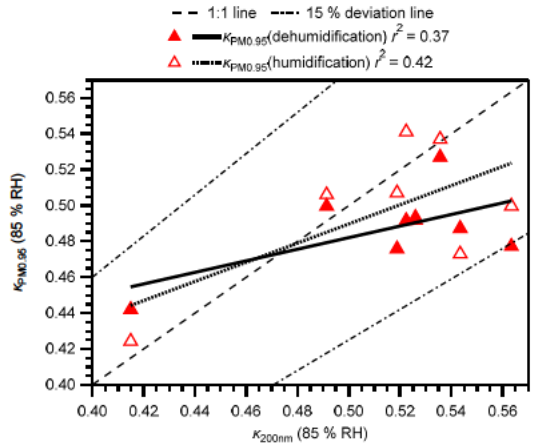

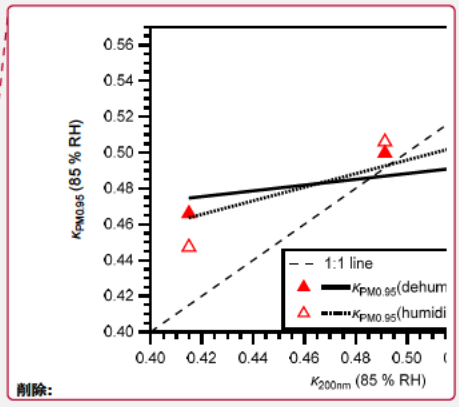

削除:

Figure 6: Comparison of calculated κ for $PM_{0.95}$ ($\kappa_{PM0.95}$) in humidification and dehumidification branches and κ for 200 nm atmospheric particles from online HTDMA analysis. Regression lines, 1:1 line, and 15 % deviation lines are also presented. It is noteworthy that online data only represent less than 2 % of the aerosols in a day, whereas offline data represent more than 95 % of aerosols in a day (10 am – 10 am).

削除: and

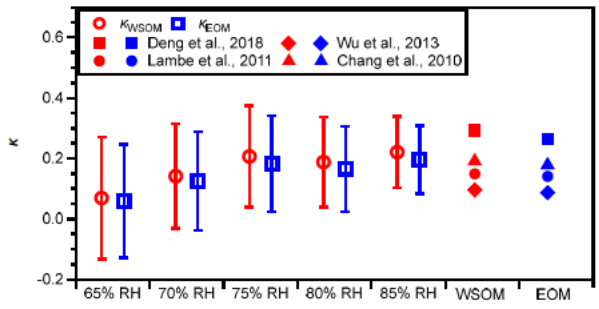

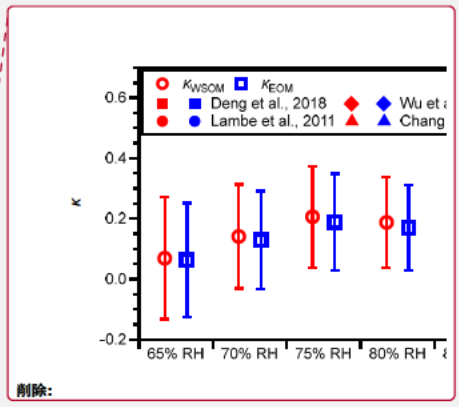

削除:

Figure 7: Estimated hygroscopicity parameter values of WSOM (κ_{WSOM}) and EOM (κ_{EOM}) under different RH conditions in dehumidification branches. Open markers present mean values. Whiskers present standard deviations of the related mean value. The hygroscopicity parameter values of WSOM and EOM predicted based on regression lines reported for the hygroscopicity

parameter values of organics and its O:C (Chang et al., 2010 (0.42 ± 0.04 % supersaturation); Lambe et al., 2011 (0.1–1.5 % supersaturation); Wu et al., 2013 (90 % RH); Deng et al., 2018 (0.11–0.80 % supersaturation)), where mean values of the O:C of WSOM (0.84, red markers) and of EOM (0.79, blue markers) were used.

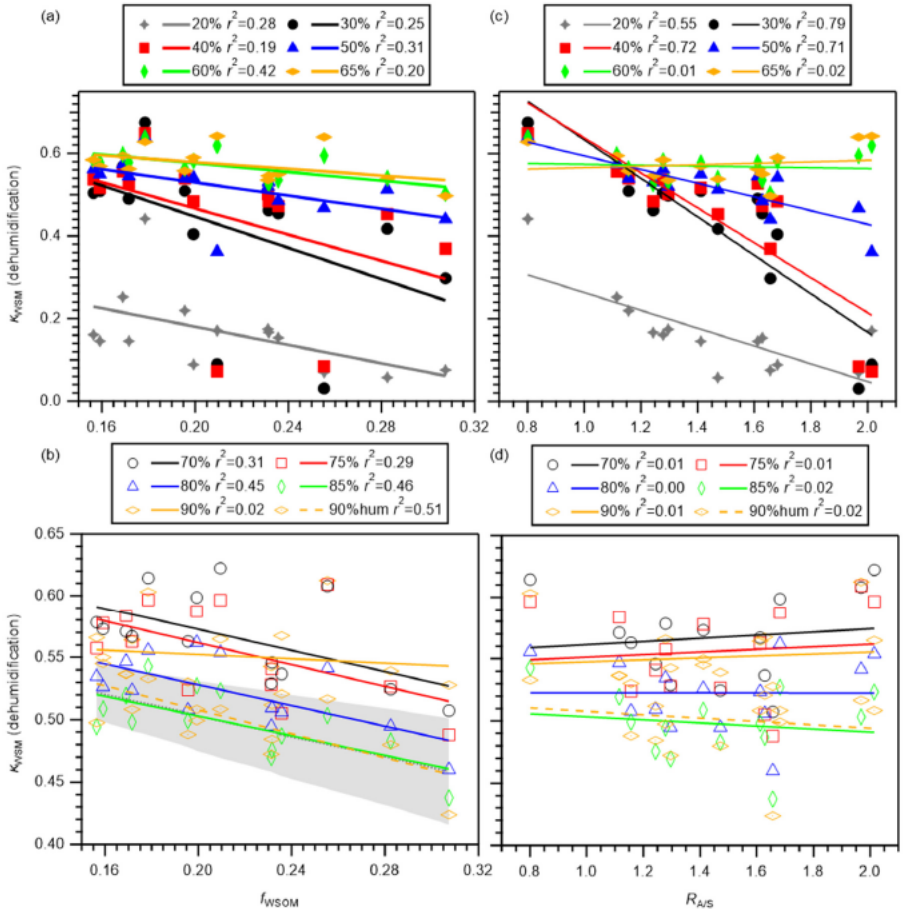

Figure 8: The κ_{WSM} values in the dehumidification branch versus (a and b) the mass fractions of WSOM in WSM (f_{WSOM}) and (c and d) the ammonium-to-remaining sulfate molar ratio ($R_{A/S}$) from the offline analysis. Panels a and c present results obtained at 20, 30, 40, 50, 60, and 65 % RH. Panels c and d present results obtained at 70, 75, 80, 85, and 90 % RH. The κ_{WSM} at 90 % RH in

删除: ;
删除: ;
删除: ;
删除:),

the humidification branch (90%hum) was also compared to (b) f_{WSOM} and (d) $R_{A/S}$. The shaded area in panel (b) show κ_{WSM} predicted by application of mean value of κ_{inorg} (0.59) and mean ± standard deviation of κ_{WSOM} for 85 % RH (0.22±0.12) using Eq. (2). Coefficients of determination r^2 are also presented.

Supplement of

Offline analysis of the chemical composition and hygroscopicity of sub-micrometer aerosols at an Asian outflow receptor site and comparison with online measurements

Yange Deng[1,2,3], Hiroaki Fujinari[1], Hikari Yai[1], Kojiro Shimada[4,5], Yuzo Miyazaki[6], Eri Tachibana[6], Dhananjay K. Deshmukh[7], Kimitaka Kawamura[7], Tomoki Nakayama[2,8], Shiori Tatsuta[4], Mingfu Cai[9,10], Hanbing Xu[9], Fei Li[11,12], Haobo Tan[11], Sho Ohata[13,14,15], Yutaka Kondo[16], Akinori Takami[17], Shiro Hatakeyama[4,18], and Michihiro Mochida[1,2]

[1] Graduate School of Environmental Studies, Nagoya University, Nagoya, 464-8601, Japan

[2] Institute for Space-Earth Environmental Research, Nagoya University, Nagoya, 464-8601, Japan

[3] Now at National Institute for Environmental Studies, Tsukuba, 305-8506, Japan

[4] Faculty of Agriculture, Tokyo University of Agriculture and Technology, Tokyo, 183-8538, Japan

[5] Now at Department of Chemistry, Biology, and Marine Science, University of the Ryukyus, Okinawa, 903-0213, Japan

[6] Institute of Low Temperature Science, Hokkaido University, Sapporo, 060-0819, Japan

[7] Chubu Institute for Advanced Studies, Chubu University, Kasugai, Aichi, 487-8501, Japan

[8] Now at Graduate School of Fisheries and Environmental Sciences, Nagasaki University, Nagasaki, 852-8521, Japan

[9] School of Atmospheric Sciences, Sun Yat-sen University, Zhuhai, Guangdong, 519082, China

[10] Now at Institute for Environmental and Climate Research, Jinan University, Guangzhou, Guangdong, 511443, China

[11] Institute of Tropical and Marine Meteorology, China Meteorological Administration, Guangzhou, 510-640, China

[12] Now at Xiamen Key Laboratory of Straits Meteorology, Xiamen Meteorological Bureau, Xiamen, 361012, China

[13] Department of Earth and Planetary Science, The University of Tokyo, Tokyo, 113-8654, Japan

[14] Now at Institute for Space-Earth Environmental Research, Nagoya University, Nagoya, 464-8601, Japan

[15] Now at Institute for Advanced Research, Nagoya University, Nagoya, 464-8601, Japan

[16] National Institute of Polar Research, Tokyo, 190-8518, Japan

[17] National Institute for Environmental Studies, Tsukuba, 305-8506, Japan

[18] Now at Asia Center for Air Pollution, Japan Environmental Sanitation Center, Niigata, 950-2144, Japan

Correspondence to: Michihiro Mochida (mochida@isee nagoya-u ac jp)

Text S1: Data screening and handling of filter samples

The RH and temperature values were recorded every 5 s during offline experiments using HTDMA. For derivation of the hygroscopic growth factors, only data obtained when the RH values at the outlet of DMA2 during a voltage scan (3 min) were used when they fulfilled the following two criteria: 1) the absolute difference between the mean and setting RH values was less than 0.5 %; 2) the absolute standard deviation of the RH values was less than 0.2 %.

Chemical analyses of OC/EC, WSOC, and ions were performed two or more times for a series of samples. Results from the last series of the analyses for all samples were regarded as the most reliable and were used for this study. As described in our earlier report, sampling of $PM_{0.95}$ on 8 × 10 inch filters accompanies high loading of aerosol samples at the corners and edges of the effective sampling area (Chen et al., 2017). At least for the last series of quantification using ion chromatograph, carbon analyzer, and TOC analyzer (for WSOC), we specifically devoted attention to avoiding the use of aerosol samples at the corners and edges of the effective sampling area. Positions of the effective sampling area were assumed to be at the center of the filters, although they must have differed slightly from sample to sample. The available record of the positions for TOC analysis is incomplete but there is no indication of the use of punches at edges/corners. Although this non-uniformity was not considered at the time of sample extraction for HTDMA and offline-AMS analyses, good agreement between the calculated atmospheric concentrations of WSOM from the TOC analysis and the OM:OC of WSOM and those from the AMS analysis alone (Text S5, Fig. S6) indicates that bias from non-uniformity, even if it exists, is expected to be slight.

削除: S5

Malfunction of the chopper in the AMS occurred during its online W-mode operation in Okinawa in the period of 28–31 October 2015. The period from the first to the last cases that airbeam correction factor was greater than 1.2 was estimated to be under the influence of the malfunction. The W-mode data during the period were excluded from the analysis. Note that, for both V- and W-modes, effective ambient measurement data were not collected temporarily also in other times during the campaign.

Text S2: Calibration of DMA size selection

Size selection of the two DMAs in the HTDMA for offline analysis was assessed by measuring the number–size distributions of 55, 100, 309, and 498 nm standard size PSL particles (models SC-0055-D, SC-0100-D, and SC-032-S, JSR, and model 3500A, Thermo Fisher Scientific Inc.) followed by determination of their mode diameters by fitting. Whereas the measured mode diameters of 100 and 309 nm PSL particles were within the prescribed expanded uncertainty ranges, the measured mode diameters of 55 and 498 nm PSL particles were greater than the upper ends of the manufacturers'

warranties: 10.4 % and 1.91 %, respectively, for 55 and 498 nm particles (Table S2). Differences for 55 and 498 nm are not expected to influence the analyses greatly because the set diameter of DMA1 was 100 nm and because the measured hygroscopic growth factors of the WSM samples were within the range of 0.98–1.88, corresponding to diameters of 98–188 nm. The size selection of SMPS for the online atmospheric measurement was also assessed by measuring the number–size distributions of 55, 100, 309, and 498 nm standard size PSL particles (models are given above). Whereas the measured mode diameters of 55 nm PSL particles were 9.6 % greater than the upper end of the manufacturer's warranty, the measured mode diameters of PSL particles with other sizes were within the ranges of the prescribed expanded uncertainty.

Text S3: Evaluation of HTDMA measurements using AS solution

To evaluate HTDMA performance for hygroscopic growth measurements, the hygroscopic growth of AS particles was measured using the HTDMA following the same procedure as that for WSM particles. Results were compared with those predicted using the E-AIM III model (Text S6, Fig. S3a). Here, the accuracy of RH measurements by Vaisala's sensors is ≤2 % according to the manufacturer's warranty. Smaller than expected deliquescence RH (DRH, between 70–75 % versus 80 % (Tang and Munkelwitz, 1994)) and efflorescence RH (ERH, approx. 30 % versus 37 % (Tang and Munkelwitz, 1994)) of AS might be the result of the history of RH in and downstream of NH2, until AS particles were transferred to DMA2 in the HTDMA. The differences provide a guide to uncertainty of the DRH and ERH measurements.

Furthermore, for AS in the humidification branch, except at 20–30 and 85 % RH, and in the dehumidification branch at 30–65 and 90 % RH, great disagreement was observed between measured and predicted κ_{AS} (predicted values deviated from those of measured ones by >15 %, Fig. S3b), which implies some bias of the measured RH and/or of analysis based on the E-AIM model. Because the differences would strongly affect quantitative analysis results if they rely on a combination of measurements and the E-AIM model, only data at 85 % RH in the humidification branch and the RH range of 65–85 % in the dehumidification branch were used to calculate the hygroscopicity parameters for WSOM (κ_{WSOM}) and EOM (κ_{EOM}). Note that the determined values of g_f were nearly unity or greater at all RH for both AS (>0.996) and WSM (>0.997) (Fig. S3 and Sect. 3.2). Therefore, there is no indication of non-sphericity of dried particles in the HTDMA (Gysel et al., 2004; Jung et al., 2011).

Text S4: Sample blank evaluation and HTDMA measurement repeatability

削除: S5

削除: S2a

削除: <

削除: %

削除: S2b

削除: The considerable disagreement at low RH might be attributable to the assumption of perfectly spherical and non-porous solid AS particles, and might also be attributable to bias of the E-AIM model and uncertainty of the RH measurements

Blank filters were extracted using the same procedure as that used for aerosol sample filters (Sect. 2.1). Volume–size distributions of the obtained WSM particles were scanned using SMPS under dry conditions. Results (Fig. S4) show that the volume concentrations of the WSM particles obtained from the blank sample were much lower than those of the aerosol samples. At the dry diameter of 100 nm, the volume concentration of WSM particles from blank samples was, on average, 1.9 % (range 0.9 %–18 %) of those from aerosol samples. These results suggest that possible interference by non-volatile contaminants is, in general, small.

删除: S3

To assess the repeatability of the HTDMA analysis, the hygroscopic growth of WSM particles from sample OKNW_035 was measured three more times in both humidification and dehumidification modes more than five months after measurement of all extracted samples. Both extraction by water and measurement by HTDMA were repeated three times. Results of the additional three measurements are presented in Fig. S5. The standard deviations of g_f in the humidification (or dehumidification) branch were 0.01 (or 0.005), 0.02 (or 0.03), and 0.04 (or 0.02) respectively at 80, 85, and 90 %. The relative standard deviations of the measured g_f were smaller than 6 %, even in the RH range of 60–75 %, where deliquescence of the WSM aerosol particles might have occurred. The values of g_f from first measurements at 80, 85, and 90% RH were larger than the mean of the three repeat measurements in the humidification (or dehumidification) branch by 5.4 (or 3.2), 4.7 (or 5.6), and 3.0 (or 7.3) %, without correction for the slight difference of the sizing (Sect. 2.2) between DMA1 and DMA2. The first measurement was not included in the repeatability analysis because a possible change of the condition of the HTDMA during the long interval might have affected the result.

删除: S4

Text S5: Quantification of WSOM and WISOM based on mass spectra

The mass concentrations of WSOM and WISOM were determined using a phthalic acid method (Han et al., 2016) as follows. The mass spectra of WSOM (or WISOM), pure phthalic acid, and the mixtures of WSOM (or WISOM) and phthalic acid were obtained from offline AMS analysis. The mass ratios of WSOM (or WISOM) to phthalic acid in the mixtures (R_m) were calculated assuming the normalized mass spectra of the mixture are linear combinations of those of WSOM (or WISOM) and pure phthalic acid. For the calculation of R_m, the same relative ionization efficiency was applied for WSOM (or WISOM) and phthalic acid. The signal at m/z 38 was excluded from the analysis for the quantification because it showed negative values and suggests that the contribution of $^{38}Ar^+$ signal was not subtracted in an appropriate quality. The mass concentration of WSOM (or WISOM) (m_{OM}, μg m^{-3}) is calculable using Eq. S1 as shown below.

$$m_{OM} = \frac{10^6 R_m C_{ph} M_{ph} M_T A_T}{100 M_{ext} A_{ext} V_T} \quad \text{(S1)}$$

Therein, C_{ph} (weight %) represents the mass concentration of phthalic acid in water (or dichloromethane/methanol) solution, M_{ph} (g) is the mass of the phthalic acid solution added to the mixture, M_{ext} (g) is the mass of the WSM (or WISOM) solution added to the mixture, M_T (g) is the total mass of the extracted WSM (or WISOM) solution, A_{ext} (cm^2) is the area of the filter used for the extraction, A_T (cm^2) is the total filter area subjected to aerosol sample collection, and V_T (m^3) is the total volume of air sampled during the aerosol collection. The mass concentration of WSOM derived here shows good agreement with that derived as the product of WSOC from the TOC analyzer and the OM:OC of WSOM (Fig. S6). The consistent result supports the propriety of the quantification of WSOM and WSOC.

删除：S5

Text S6: Hygroscopic growth of WSM predicted using the E-AIM model

Hygroscopic growth of WSM without consideration of water uptake by WSOM and that of ammonium sulfate (AS) particles as a function of water activity (a_w) at 0.10 to 0.99, and also the corresponding hygroscopicity parameter (κ) were derived based on the output of the online E-AIM III model and the κ- Köhler theory as described below.

For application of the E-AIM III model to WSM, ammonium, sodium, and sulfate among quantified anions were considered because the concentrations of other ions were low (Table 3). Excess anions in each WSM solution were assumed to be in balance with protons electrically. The a_w range of 0.10–0.99 at a resolution of 0.01 was applied to each WSM solution and the AS solution at 298.15 K. In all calculations, the partitioning of HNO_3, HCl, H_2SO_4, and NH_3 to the gas phase was prevented. Furthermore, for the dehumidification branch, the formation of solids was also prevented. The quantity of water as a function of a_w in thermodynamically equilibrium conditions was obtained from the model. The hygroscopic growth factor was calculated as the ratio of the sum of the volumes of water and dry WSM (or AS) particle to the volume of dry WSM (or AS) particle. The volumes of dry WSIM and WSOM were calculated in the same manner as that stated in Text S7. The hygroscopicity parameter of WSM (κ_{WSM}), WSIM (κ_{inorg}), and AS (κ_{AS}) was derived following Eq. 2 in Petters and Kreidenweis (2007).

For WSM particles from atmospheric samples, the exponential part of the κ- Köhler equation, which represents the curvature (Kelvin) effect, was calculated on the assumption that the surface tension is that of pure water, the partial molar volume of water in the solution is equal to that of pure water, and

that the volumes of WSOM in the particles were considered whereas the water uptake by the WSOM component was ignored. In the case of AS particles, the surface tension of the solution obtained from the E-AIM model was used instead for the calculation. The RH above the particle surface was then calculated as the product of a_w and the corresponding exponential part. The κ_{WSM} and κ_{inorg} (or κ_{AS}) at the measured RH (i.e., 20, 30, 40, 50, 60, 65, 70, 75, 80, 85, and 90 %) were determined by looking up the a_w-κ_{WSM}-κ_{inorg}-RH (or a_w-κ_{AS}-RH) table at a resolution of 0.01.

Text S7: Derivation of volume concentrations of WSIM, WSOM, WISOM, and EC in $PM_{0.95}$

The chemical composition obtained from the offline analysis (Sect. 2.3) was used to derive the volume concentrations of WSIM, WSOM, WISOM, and EC for reconstruction of the hygroscopicity of WSOM, EOM and $PM_{0.95}$. To ascertain the volume concentration of WSIM, the respective contributions from potassium, calcium, magnesium, nitrate, and chloride were ignored because their contributions were minimal compared to those of sulfate, ammonium, and sodium (Table S3). Furthermore, sulfate in the dry condition was assumed to be present preferentially in the form of sodium sulfate (Na_2SO_4). The remaining sulfate was assumed to be present in the form of ammonium sulfate (AS, $(NH_4)_2SO_4$), letovicite (LET, $(NH_4)_3H(SO_4)_2$), ammonium hydrogen sulfate (AHS, NH_4HSO_4), and/or sulfuric acid (SA, H_2SO_4) according to the molar ratios of ammonium to the remaining sulfate ($R_{A/S}$) as follows: ammoniated sulfate was in the form of AS and LET for $1.5<R_{A/S}\leq2$, in the form of LET and AHS for $1<R_{A/S}\leq1.5$, and in the form of SA and AHS for $0<R_{A/S}\leq1$. The volume concentration of WSOM (or WISOM) was found as the ratio of its mass concentration to its density calculated using its O:C and H:C from the offline AMS analysis. The volume concentration of EOM was equal to the sum of the volume concentrations of WSOM and WISOM. The volume concentration of WSM was inferred as the sum of the volume concentrations of WSIM and WSOM. The volume concentration of EC was found using the EC mass concentration from OC/EC analysis, with the assumed density of 1.77 g cm^{-3} (Park et al., 2004).

削除: ----------改ページ----------

¶
¶
¶

Text S8: Comparisons between offline and online analyses based on organic mass spectra

Mass spectra of organics at m/z 43, 44, 55, and 57, and the atomic ratios of O to C and H to C are commonly used to characterize the aging and source characteristics of OA. Whereas the comparison between offline and online analyses of O:C is made in Sect. 3.1, here, the mass fractions of m/z 43 (or m/z 44) in organics, f_{43} (or f_{44}), the ratio of the mass fraction of m/z 55 in organics to that of m/z 57 (f_{55}/f_{57}), and H:C between offline and online analyses were compared. The results are presented in Fig. S9. For the days when the mass concentration of organics was high ($m_{OA,online} > 0.2$ µg m^{-3}), the offline

and online data are in general in good agreement. However, for the last three days when the mass concentrations of organics were low, the agreement was poor. The poor agreement may be originated from low organic mass concentrations, which should accompany relatively large uncertainty in the mass spectra. It is suggested from the result in Fig. S10: f_{44} (or H:C) from the online analysis seems sensitive to the subtraction of the contribution of CO_2 in air from the signal at m/z 44 or that of the fragment CO_2^+ when the organic mass concentration was small. Note that the signal at m/z 38 was excluded from the analysis here because $^{38}Ar^+$ from Ar carrier gas presumably influenced it.

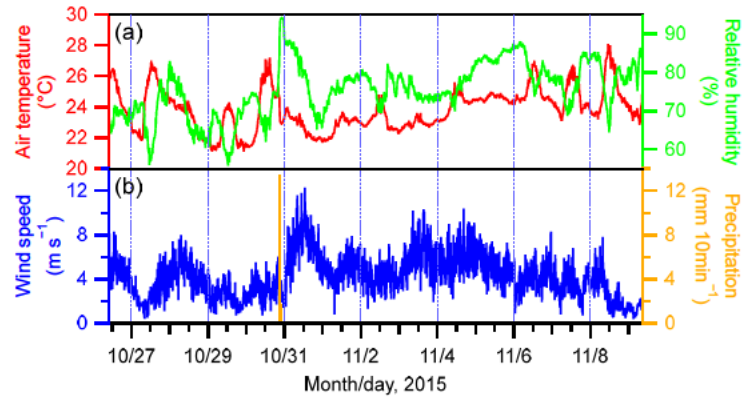

Figure S1: Time series of air temperature (°C), relative humidity (%), wind speed (m s^{-1}), and precipitation (mm 10-min^{-1}) during the sampling period for $PM_{0.95}$.

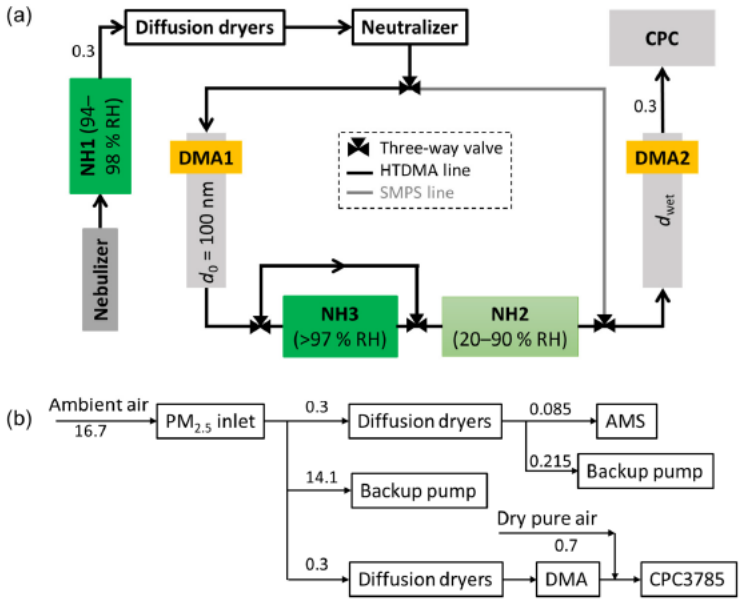

Figure S2: Schematics of the experimental set-up for (a) the offline hygroscopic growth measurements and (b) online AMS/SMPS analyses. Flow rates are in the unit of L min^{-1}. DMA: differential mobility analyzer; CPC: condensation particle counter; NH: Nafion humidifier; AMS: aerosol mass spectrometer.

削除:
Figure S2

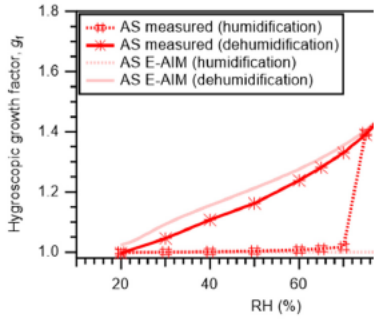

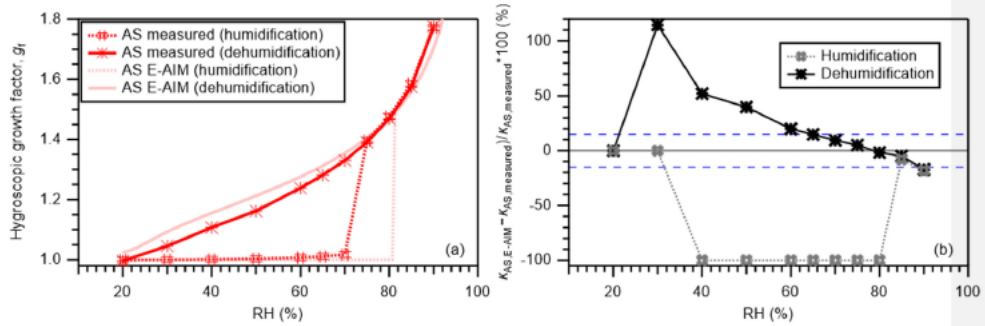

Figure S3: (a) Measured g_f and those predicted based on E-AIM in humidification and dehumidification branches for 100 nm ammonium sulfate (AS) particles. The predicted g_f in the dehumidification branch was obtained based on the assumption that solid salts are not formed. (b) Relative deviation of predicted κ_{AS} ($\kappa_{AS,E\text{-}AIM}$) from measured κ_{AS} ($\kappa_{AS,measured}$) in humidification and dehumidification branches. In both panels, markers represent individual data; lines are used to connect individual data points. The E-AIM predicted results in panel (a) are presented only by lines between points. Blue dashed lines in panel (b) represent +15 % and −15 %.

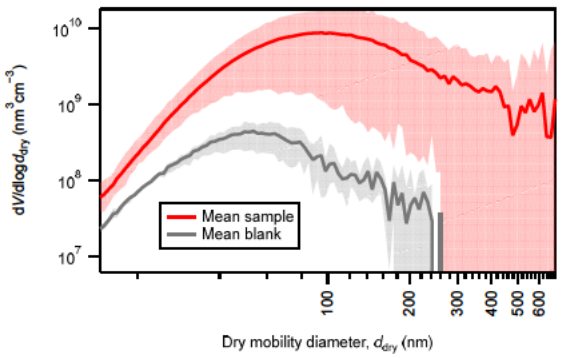

Figure S4: Volume–size distributions of WSM particles generated from ambient aerosol samples and blank samples. The red solid curve and shaded area respectively represent the means and ranges for all ambient aerosol samples. The gray solid curve and shaded area respectively represent the means and ranges of blank samples. Data below the range of the vertical axis are not shown.

删除: S3

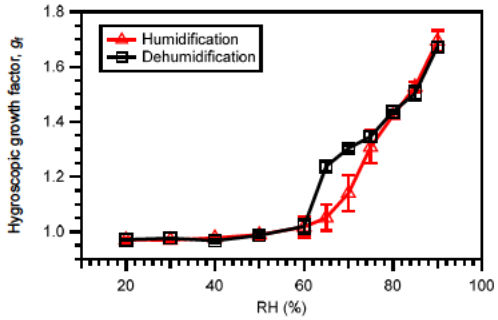

Figure S5: Results representing the repeatability of hygroscopic growth factor measurements: the g_f of 100 nm WSM particles from sample OKNW_035 as a function of RH. Markers and whiskers respectively represent mean values and standard deviations from three measurements (Text S4). The g_f values presented here are not corrected for the slight difference of the sizing (Sect. 2.2) between DMA1 and DMA2.

削除：S4

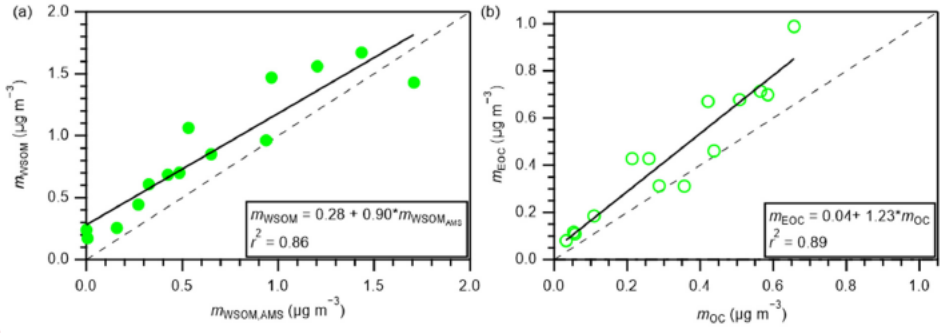

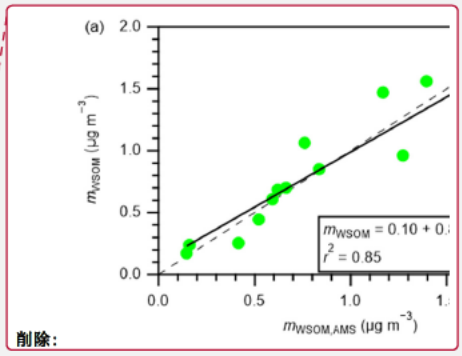

削除：

Figure S6: (a) Comparison of the mass concentrations of WSOM derived from WSOC from the TOC analyzer and the AMS-derived OM:OC of WSOM (m_{WSOM}; Sect. 2.3), and those of WSOM from the AMS analysis using phthalic acid as the internal standard ($m_{WSOM,AMS}$; Text S5). (b) Comparison of the mass concentrations of EOC (m_{EOC}) from offline AMS analysis and those of OC (m_{OC}) from the thermal analysis. In both panels, solid and dashed lines respectively represent regression lines and 1:1 lines.

削除：S5

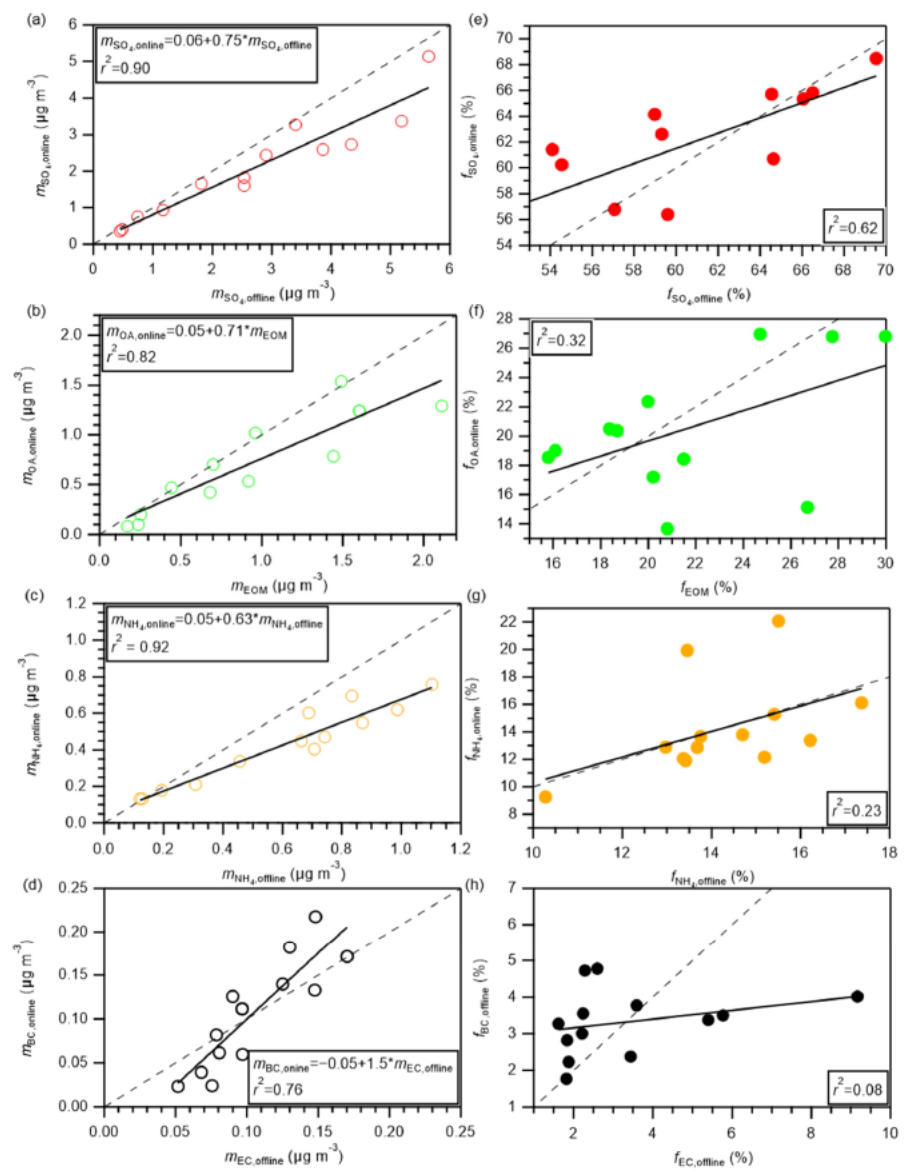

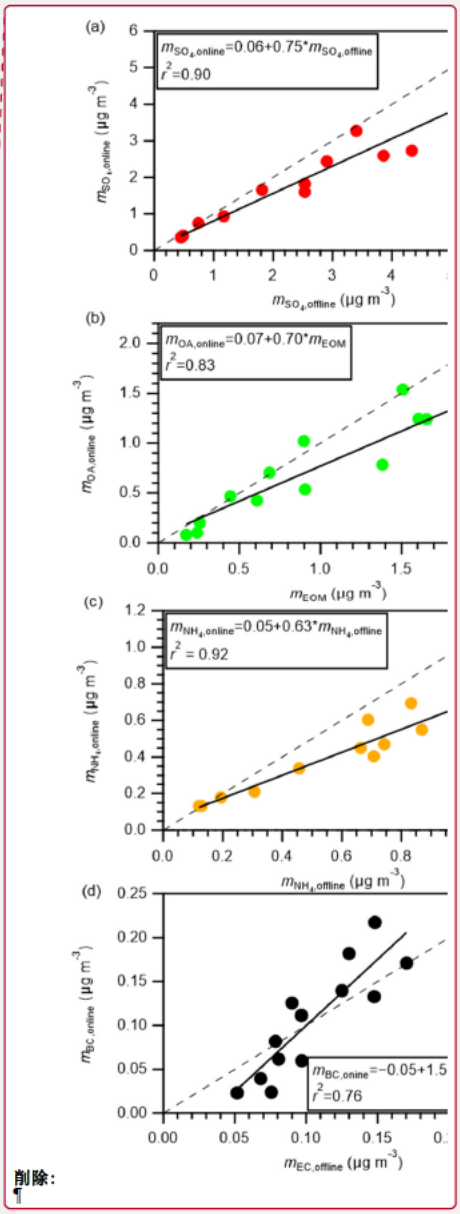

削除:

Figure S7: Comparison of the mass concentrations/fractions of chemical components in aerosols obtained from online and offline analyses: (a) mass concentrations of sulfate from online AMS analysis ($m_{SO4,online}$) versus those from offline IC analysis ($m_{SO4,offline}$); (b) mass concentrations of organics from

削除: S6

online AMS analysis ($m_{OA,online}$) and those from offline analysis (m_{EOM}); (c) mass concentrations of ammonium from online AMS analysis ($m_{NH4,online}$) versus those from offline IC analysis ($m_{NH4,offline}$); (d) mass concentrations of BC from online COSMOS analysis ($m_{BC,online}$) versus those from offline thermal analysis ($m_{EC,offline}$); (e) mass fractions of sulfate in the total mass of SO_4, EOM, NH_4, and BC from online analyses ($f_{SO4,online}$) versus those in the total mass of SO_4, OA, NH_4, and EC from the offline analyses ($f_{SO4,offline}$); (f) mass fractions of organics in the total mass of SO_4, EOM, NH_4, and BC from the online analyses ($f_{OA,online}$) versus those in the total mass of SO_4, OA, NH_4, and EC from offline analyses (f_{EOM}); (g) mass fractions of ammonium in the total mass of SO_4, EOM, NH_4, and BC from online analyses ($f_{NH4,online}$) versus those in the total mass of SO_4, OA, NH_4, and EC from offline analyses ($f_{NH4,offline}$); (h) mass fractions of BC in the total mass of SO_4, EOM, NH_4, and BC from online analyses ($f_{BC,online}$) versus those in the total mass of SO_4, OA, NH_4, and EC from offline analyses ($f_{EC,offline}$). Solid and dashed lines respectively show regression lines and 1:1 lines.

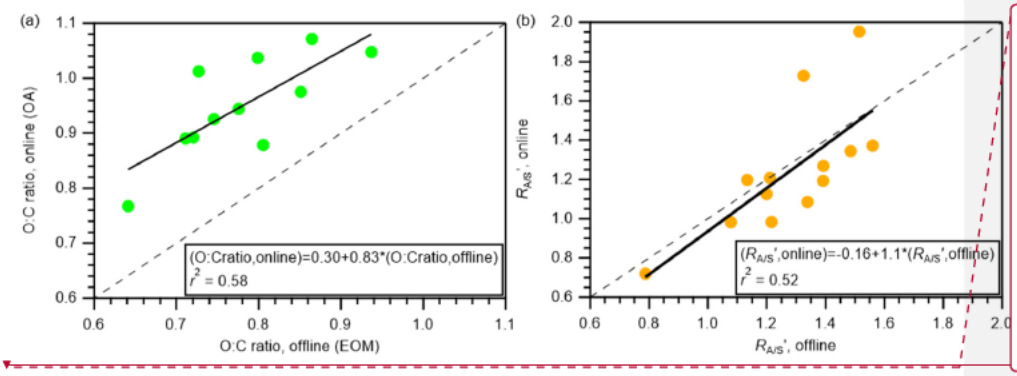

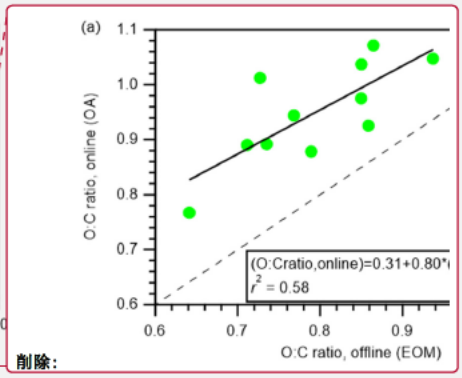

削除：

Figure S8: (a) Comparison of the O:C of OA from online analysis to those of EOM from offline analysis. (b) Comparison of the ammonium to sulfate ratio ($R_{A/S}'$) from online and offline analyses (Sect. 3.1). Solid and dashed lines respectively represent regression lines and 1:1 lines.

削除：S7

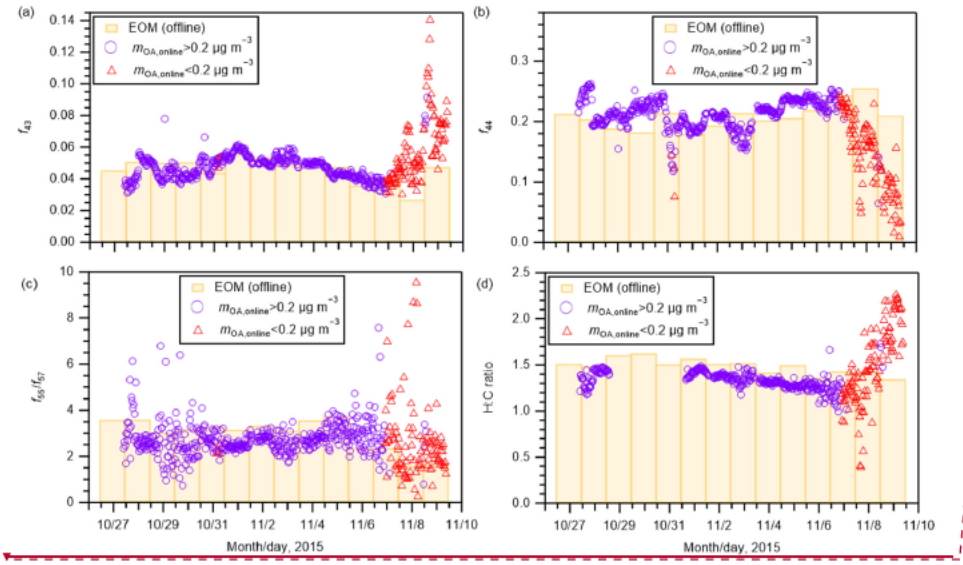

Figure S9: Comparisons between offline and online results of (a) f_{43}, (b) f_{44}, (c) f_{55}/f_{57}, and (d) H:C from the mass spectral analyses for EOM (offline) and organic aerosol (online). Data from offline analysis are presented as bars and those from online analysis for the cases of $m_{OA,online} > 0.2$ μg m^{-3} and $m_{OA,online} < 0.2$ μg m^{-3} ($m_{OA,online}$: mass concentrations of organic aerosol from the online analysis) are presented as open circles and open triangles, respectively. In panel (c), online data with values greater than 10 or smaller than 0 are not presented.

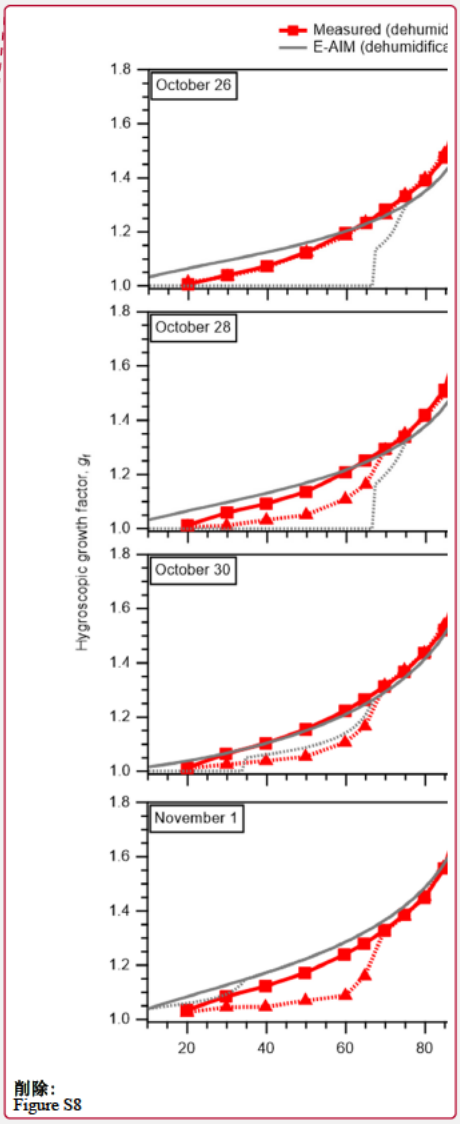

削除:
Figure S8

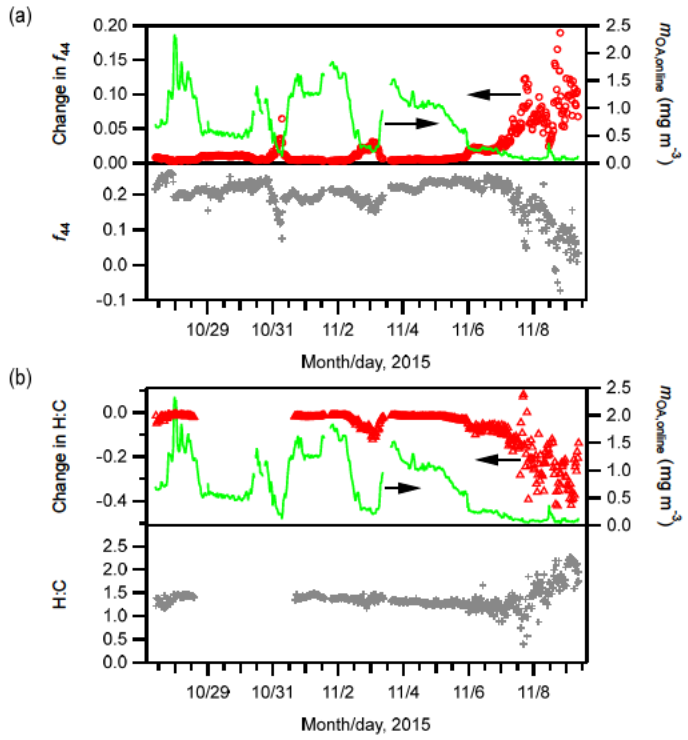

Figure S10: (a) Time series of online f_{44} with fragCO2[44] used for the analyses in this study and the changes in f_{44} (open circles) in the case that 10% lower fragCO2[44] values are used. (b) Time series of online H:C with HR_frag_air[{CO2}] used for the analyses in this study and the changes in H:C (open triangles) in the case that 20% lower HR_frag_air[{CO2}] values are used. The time series of the mass concentrations of organic aerosol from the online analysis ($m_{OA,online}$, green lines) are also shown in both panels.

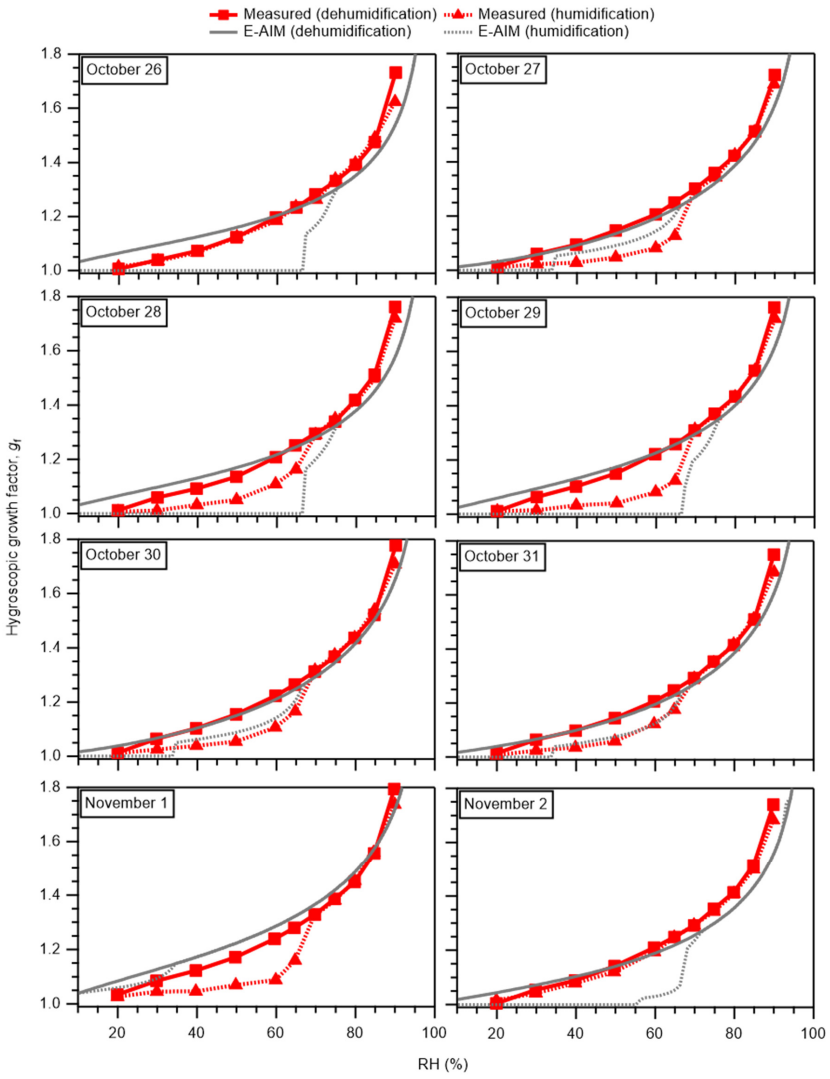

Figure S11: The g_f of 100 nm WSM particles in humidification and dehumidification branches as a function of RH for individual samples. The g_f predicted from the E-AIM model without considering the water retained by WSOM are also presented. Dates shown on panels represent dates when sampling started.

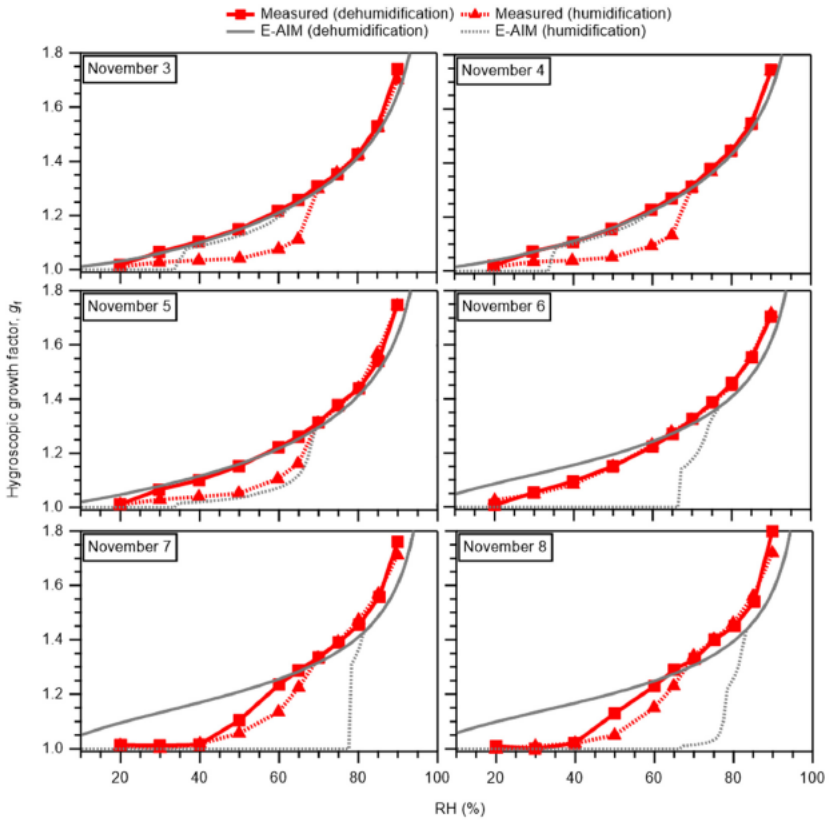

Figure S11 (continued)

删除：S8

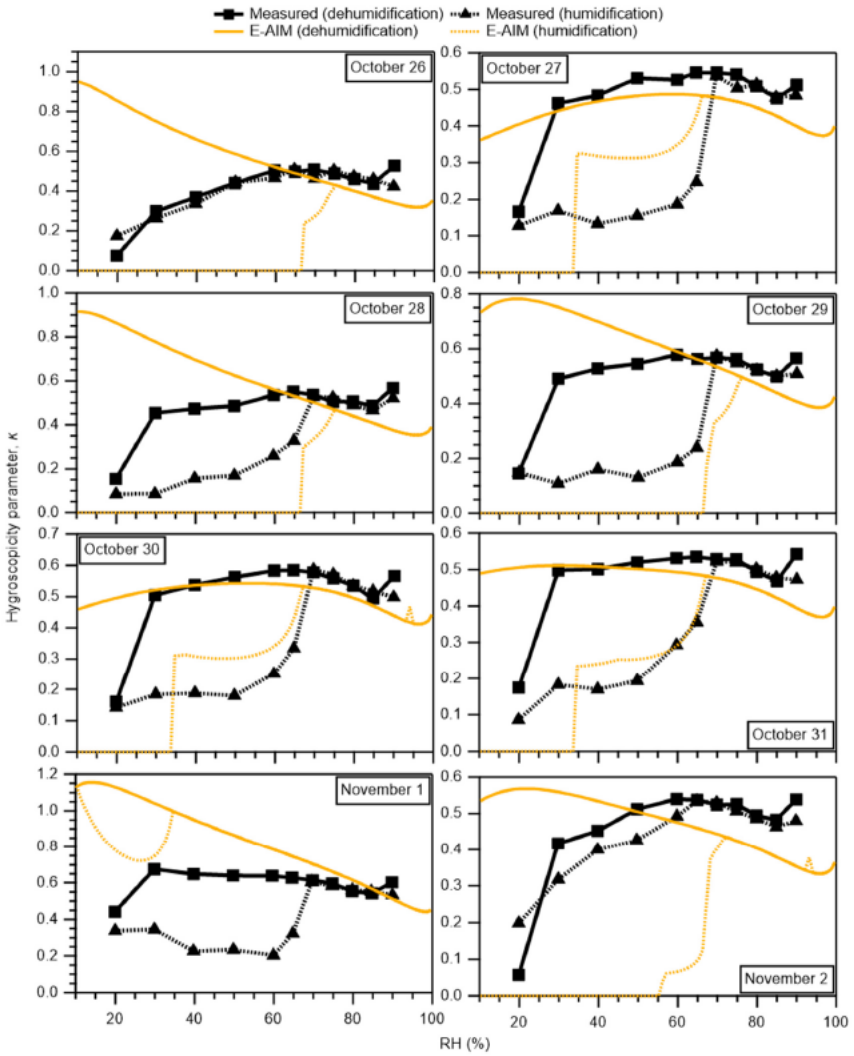

Figure S12: The κ_{WSM} of 100 nm WSM particles in humidification and dehumidification branches as a function of RH. The κ_{WSM} values predicted from the E-AIM model without consideration of water retained by WSOM are also shown. Dates shown on panels represent dates when sampling started.

删除：S9

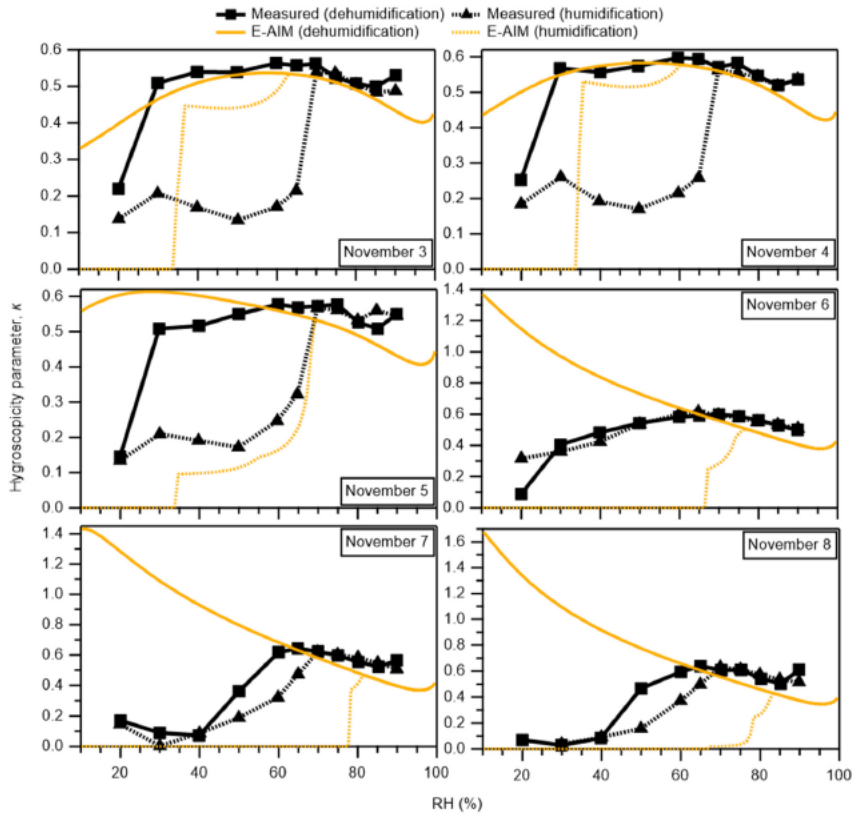

Figure S12 (continued)

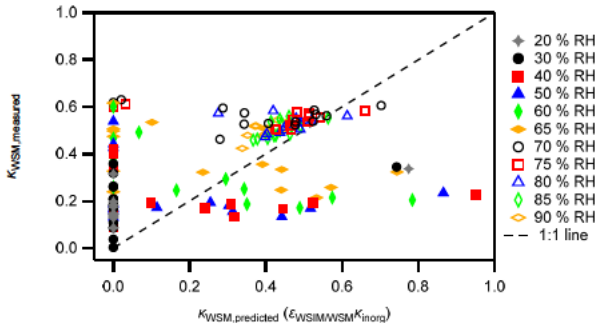

Figure S13: Measured versus predicted κ_{WSM} at different RH in the humidification branch. The dashed line is the 1:1 line.

删除：S9

删除：¶

删除：S10

删除：

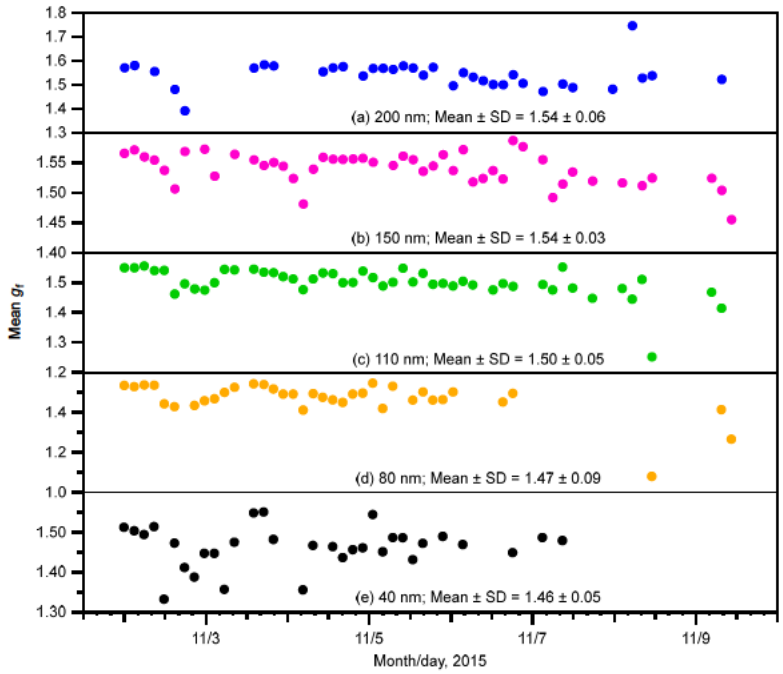

Figure S14: Time series of mean g_f for aerosol particles with different dry diameters. The mean ± SD values for the entire observation period are also presented.

削除：¶

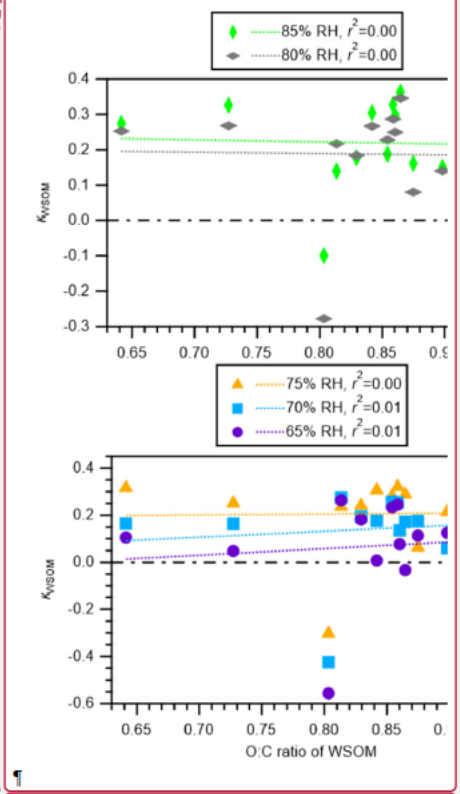

¶

削除：S11

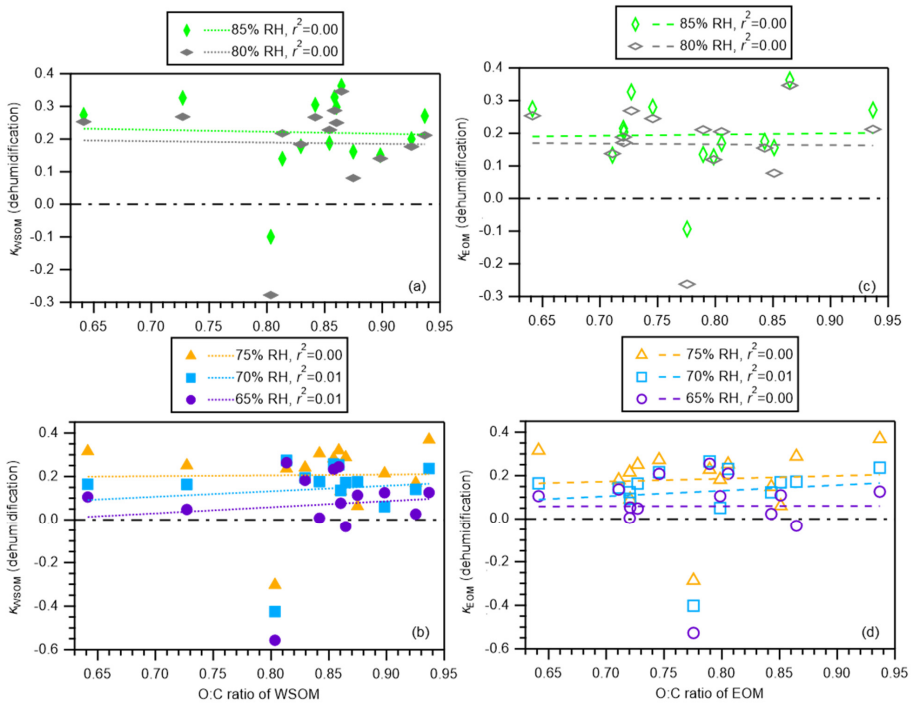

Figure S15: (a and b) Scatter plots of κ_{WSOM} in the dehumidification branch versus O:C of WSOM at (a) 80 and 85 % RH and at (b) 65, 70, and 75 % RH. (c and d) Scatter plots of κ_{EOM} in the dehumidification branch versus O:C of EOM at (c) 80 and 85 % RH and at (d) 65, 70, and 75 % RH.

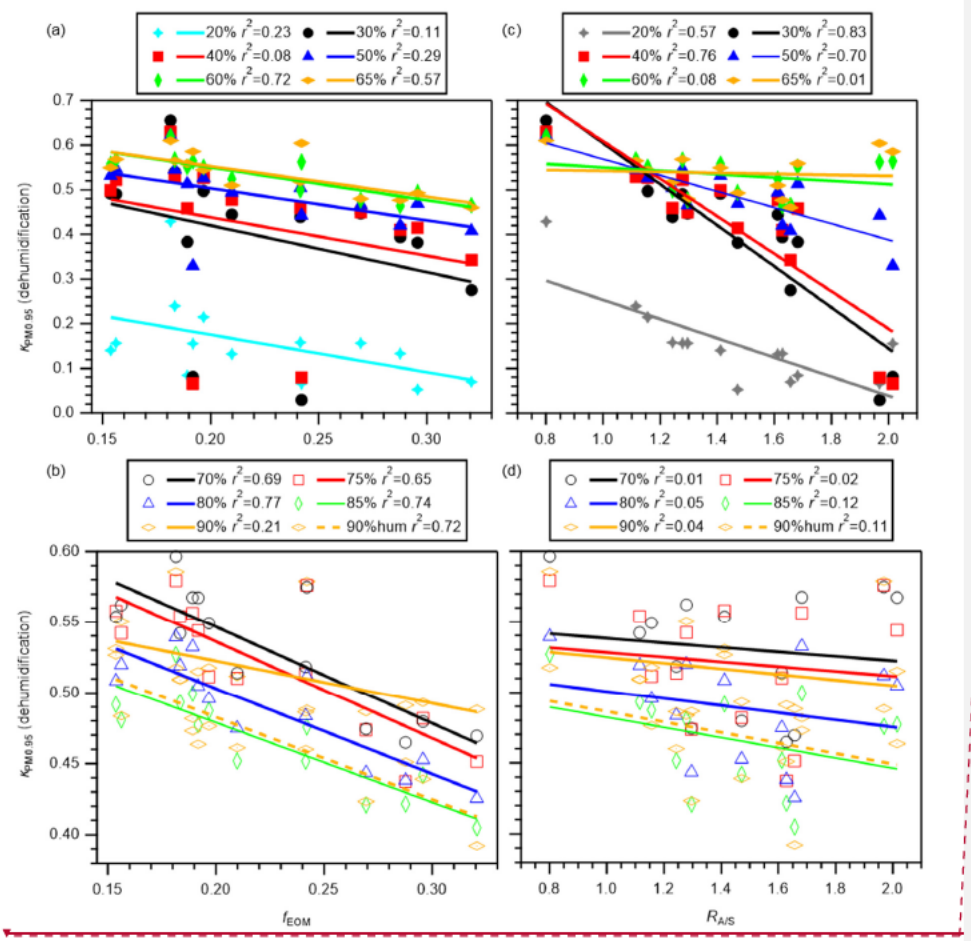

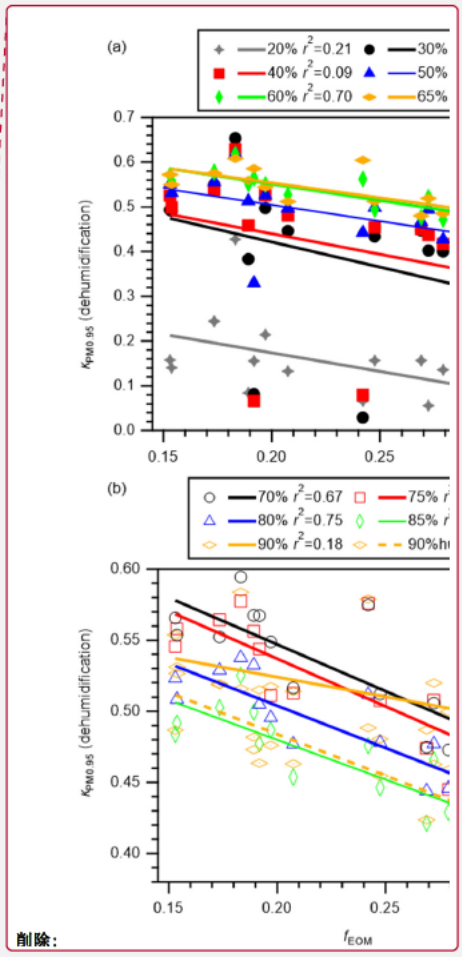

削除:

Figure S16: The $\kappa_{PM0.95}$ values in the dehumidification branch versus (a and b) mass fractions of EOM in PM0.95 (f_{EOM}) and (c and d) the ammonium-to-remaining sulfate molar ratio ($R_{A/S}$) from offline analysis. Panels a and c present results obtained for 20, 30, 40, 50, 60, and 65 % RH. Panels c and d present results obtained for 70, 75, 80, 85, and 90% RH. The $\kappa_{PM0.95}$ at 90 % RH in the humidification branch (90%hum) was also compared to (b) f_{WSOM} and (d) $R_{A/S}$. Coefficients of determination r^2 are also presented.

削除: S12

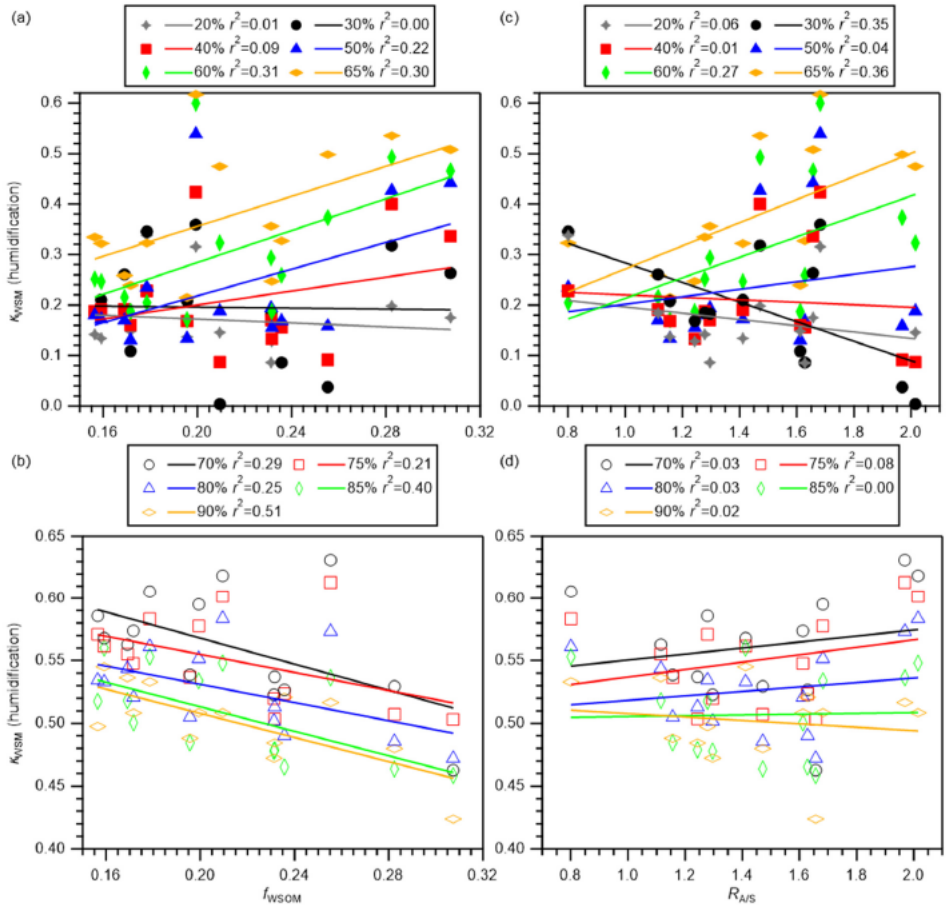

Figure S17: The κ_{WSM} values in the humidification branch versus (a and b) mass fractions of WSOM in WSM (f_{WSOM}) and (c and d) the ammonium-to-remaining sulfate molar ratio ($R_{A/S}$) from offline analysis. Panels a and c present results obtained for 20, 30, 40, 50, 60, and 65 % RH. Panels c and d present results obtained for 70, 75, 80, 85, and 90 % RH. Coefficients of determination r^2 are also shown.

删除：S13

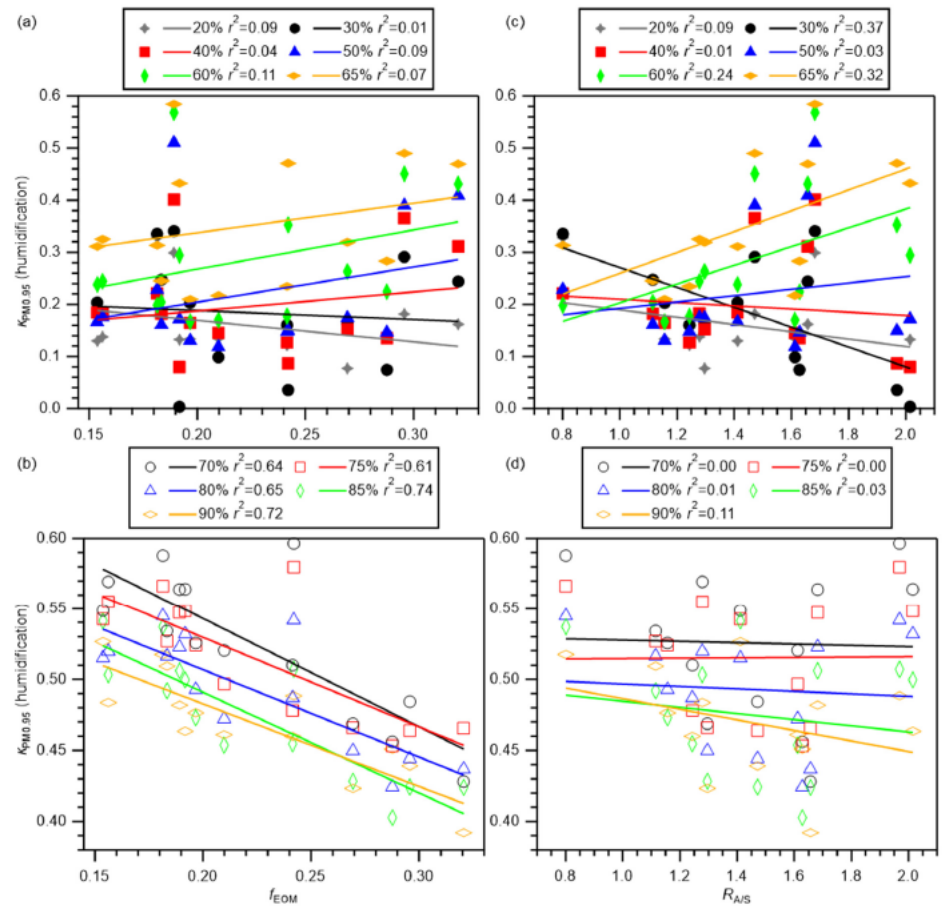

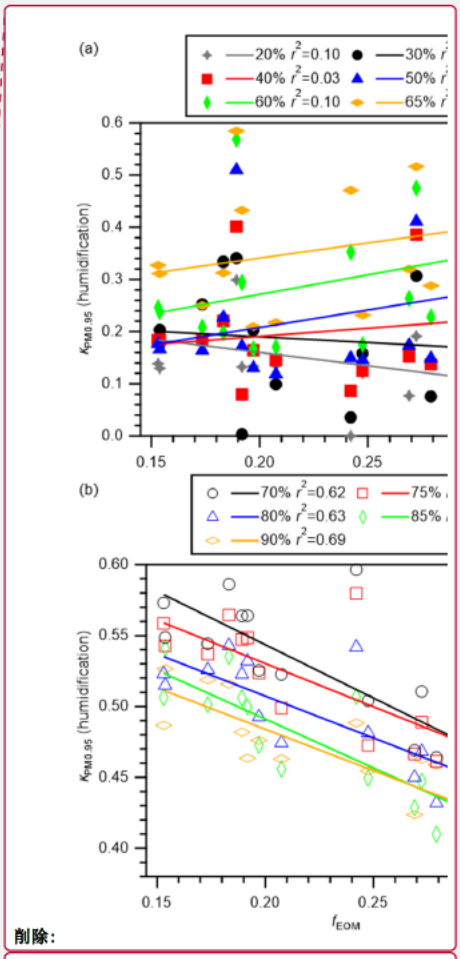

Figure S18: The $\kappa_{PM0.95}$ values in the humidification branch versus (a and b) the mass fractions of EOM in $PM_{0.95}$ (f_{EOM}) and (c and d) the ammonium-to-remaining sulfate molar ratio ($R_{A/S}$) from offline analysis. Panels a and c present results obtained for 20, 30, 40, 50, 60, and 65 % RH. Panels c and d present results obtained for 70, 75, 80, 85, and 90 % RH. Coefficients of determination r^2 are also presented.

削除:

削除: S14

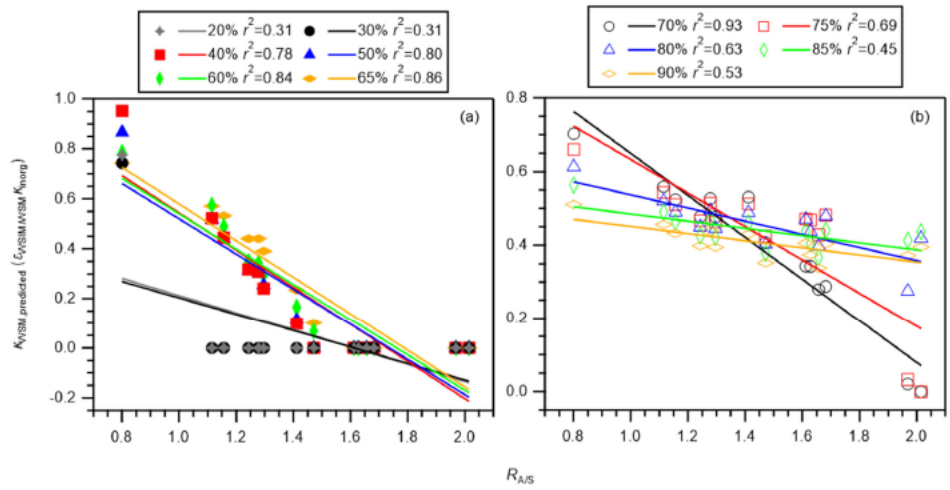

Figure S19: Scatter plots of predicted κ_{WSM} versus $R_{A/S}$ of WSM at (a) 20, 30, 40, 50, 60, and 65 % RH and (b) 70, 75, 80, 80, and 90 % RH. Markers and lines respectively represent individual data and regression lines. Coefficients of determination are also presented.

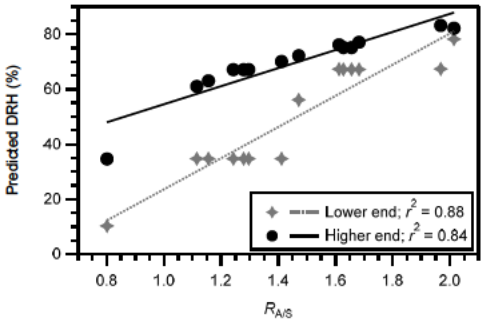

Figure S20: Scatter plots of DRH predicted by E-AIM versus $R_{A/S}$ of WSM. Gray stars present the predicted RH at which the g_f in the humidification branch became greater than unity (lower end), and the dotted line represents the corresponding regression line. Black circles show the predicted RH at which the g_f in the humidification and dehumidification branches became identical (higher end), and the solid line represents the corresponding regression line.

削除: S15

削除: S16

削除: ,

削除: solid

削除: ,

削除: dotted

Table S1: Sampling periods and sampled air volumes for the $PM_{0.95}$ studied

Sample ID	Period (in 2015, JST)	Air volume (m^3)
OKNW_001	26 Oct, 09:56:00 – 27 Oct, 09:00:03	1569.5
OKNW_003	27 Oct, 09:26:00 – 28 Oct, 09:00:00	1602.9
OKNW_005B*	28 Oct, 09:11:11 – 28 Oct, 09:11:21	0
OKNW_006	28 Oct, 09:43:30 – 29 Oct, 09:00:00	1584.5
OKNW_009	29 Oct, 09:24:00 – 30 Oct, 09:00:00	1608.7
OKNW_011	30 Oct, 09:23:00 – 31 Oct, 09:00:00	1612.5
OKNW_014	31 Oct, 09:46:00 – 1 Nov, 09:00:00	1588.1
OKNW_017	1 Nov, 09:34:10 – 2 Nov, 09:00:01	1602.8
OKNW_019B*	2 Nov, 09:39:00 – 2 Nov, 09:39:10	0
OKNW_020	2 Nov, 09:59:45 – 3 Nov, 09:00:00	1574.7
OKNW_023	3 Nov, 09:20:00 – 4 Nov, 09:00:00	1621.2
OKNW_025	4 Nov, 09:22:40 – 5 Nov, 09:00:00	1619.9
OKNW_028	5 Nov, 09:44:40 – 6 Nov, 09:00:00	1595.9
OKNW_045B*	6 Nov, 09:19:20 – 6 Nov, 09:19:30	0
OKNW_032	6 Nov, 09:49:30 – 7 Nov, 09:00:00	1590.7
OKNW_035	7 Nov, 09:24:40 – 8 Nov, 09:00:02	1619.8
OKNW_037	8 Nov, 09:25:00 – 9 Nov, 09:00:00	1620.2
OKNW_039B*	9 Nov, 09:16:00 – 9 Nov, 09:16:10	0

* Field blanks

Table S2: Mode diameters of PSL size standards measured using DMA1, DMA2, and SMPS (in nm)[a]

Manufacturer's warranty[b]	HTDMA		Online SMPS	
	DMA1	DMA2		
55 (± 1)	-	61.8 ± 0.3	60.3 ± 0.2	
100 (± 3)	100.8 ± 0.0	103.2 ± 0.2	102.8 ± 0.3	
309 (± 9)	303.3 ± 0.2	314.8 ± 1.1	307.5 ± 0.2	(308.4 ± 0.3)
498 (± 9)	-	516.7 ± 1.2	503.4 ± 0.5	

[a] The mean ± SD of the mode diameters from fittings. Results are based on calibrations done before analysis of atmospheric samples, except for the case of 309 nm PSL size standards from the SMPS, for which calibration was also made after sample analysis (in parenthesis).

[b] Mean diameter (± expanded uncertainty; $k = 2$).

Table S3: Mass concentrations of water-soluble ions (μg m^{-3}) and water-soluble organic carbon (WSOC, μgC m^{-3}) in $PM_{0.95}$[a]

Sample ID	MSA	Cl^-	NO_3^-	SO_4^{2-}	NH_4^+	Na^+	K^+	Ca^{2+}	Mg^{2+}	WSOC
OKNW_001	0.0107	BDL	0.0033	1.5761	0.4333	0.0877	0.045	0.0079	0.0118	0.4022
OKNW_003	0.0316	BDL	0.0035	3.8618	0.8696	0.0656	0.0594	0.0105	0.0099	0.6412
OKNW_006	0.025	0.0017	0.0063	2.5378	0.7076	0.1069	0.0519	0.0224	0.0147	0.4613
OKNW_009	0.0157	BDL	0.0025	2.5371	0.743	0.0396	0.0418	0.0126	0.0053	0.3079
OKNW_011	0.0154	BDL	0.0015	2.9046	0.6634	0.0677	0.0415	0.0087	0.0089	0.3015
OKNW_014	0.0413	0.0012	0.0091	4.3392	0.9866	0.1371	0.0482	0.0124	0.0194	0.7385
OKNW_017	0.0425	BDL	0.0052	5.6403	0.8334	0.0475	0.0327	0.0068	0.0091	0.6412
OKNW_020	0.0098	0.0016	0.0043	1.1744	0.3069	0.0306	0.0152	0.0063	0.0049	0.2646
OKNW_023	0.0399	0.0006	0.0054	5.1817	1.1029	0.0483	0.0592	0.0063	0.0068	0.673
OKNW_025	0.0249	BDL	0.0019	3.3991	0.6882	0.0536	0.0301	0.0057	0.0077	0.3632
OKNW_028	0.0209	BDL	0.0017	1.8159	0.4562	0.0453	0.0165	0.0059	0.0055	0.1845
OKNW_032	0.0109	BDL	0.0008	0.7429	0.1942	0.0613	0.0108	0.0053	0.0074	0.1091
OKNW_035	0.0054	BDL	0.0006	0.4499	0.1279	0.0535	0.0056	0.0044	0.0054	0.0796
OKNW_037	0.0074	0.0006	0.0018	0.4839	0.1204	0.0757	0.0042	0.0047	0.0051	0.1169
Mean	0.0215	0.0059	0.0034	2.6175	0.5881	0.0657	0.0330	0.0086	0.0087	0.3775

[a] Data were corrected for field blanks. BDL, below detection limit (i.e., mean + three times standard deviation of blank samples).

Table S4: Summary of offline measurements

Instrument	Observed component/property
HTDMA	g_E of WSM at 20, 30, 40, 50, 60, 65, 70, 75, 80, 85, and 90 RH in humidification and dehumidification branches
IC	SO_4^{2-}, NO_3^-, Cl^-, NH_4^+, Na^+, K^+, Ca^{2+}, Mg^{2+}, and MSA
TOC	WSOC and WSOM (also from AMS-derived OM:OC)
AMS	O:C, H:C, OM:OC, densities of WSOM and WISOM, WISOM, EOM, WISOC, and EOC
Carbon analyzer	OC and EC

削除： ---------- 改ページ ----------
¶

Table S5: Mean ± standard deviation of g_f, κ_{WSM}, $\kappa_{PM0.95}$, κ_{WSOM}, and κ_{EOM} in humidification and dehumidification branches

RH (%)	Humidification					Dehumidification				
	g_f	κ_{WSM}	$\kappa_{PM0.95}$	κ_{WSOM}	κ_{EOM}	g_f	κ_{WSM}	$\kappa_{PM0.95}$	κ_{WSOM}	κ_{EOM}
20	1.01±0.01	0.17±0.08	0.16±0.07	-	-	1.01±0.01	0.17±0.10	0.16±0.10	-	-
30	1.03±0.01	0.20±0.11	0.18±0.10	-	-	1.05±0.02	0.42±0.18	0.40±0.17	-	-
40	1.04±0.02	0.21±0.10	0.20±0.10	-	-	1.09±0.03	0.45±0.17	0.42±0.16	-	-
50	1.07±0.04	0.24±0.13	0.22±0.12	-	-	1.14±0.02	0.52±0.07	0.49±0.07	-	-
60	1.13±0.05	0.30±0.13	0.28±0.12	-	-	1.22±0.01	0.57±0.04	0.53±0.05	-	-
65	1.18±0.05	0.38±0.13	0.35±0.12	-	-	1.26±0.02	0.57±0.04	0.54±0.05	0.07±0.20	0.06±0.19
70	1.31±0.02	0.56±0.05	0.53±0.05	-	-	1.31±0.02	0.57±0.04	0.53±0.04	0.14±0.17	0.13±0.16
75	1.36±0.02	0.55±0.04	0.52±0.04	-	-	1.37±0.02	0.56±0.04	0.52±0.05	0.21±0.17	0.18±0.16
80	1.43±0.02	0.53±0.03	0.49±0.04	-	-	1.43±0.02	0.52±0.03	0.49±0.04	0.19±0.15	0.17±0.14
85	1.53±0.03	0.51±0.04	0.47±0.04	0.26±0.15	0.24±0.16	1.53±0.02	0.50±0.03	0.47±0.03	0.22±0.12	0.20±0.11
90	1.71±0.03	0.50±0.03	0.47±0.04	-	-	1.75±0.03	0.55±0.03	0.52±0.03	-	-

Table S6: Fractional contribution of WSOM to the κ values of WSM and $PM_{0.95}$ (mean ± standard deviation, %)

RH (%)	Humidification		Dehumidification	
	$(\varepsilon_{WSOM/WSM}\times\kappa_{WSOM})/\kappa_{WSM}\times100$	$(\varepsilon_{WSOM/PM0.95}\times\kappa_{WSOM})/\kappa_{PM0.95}\times100$	$(\varepsilon_{WSOM/WSM}\times\kappa_{WSOM})/\kappa_{WSM}\times100$	$(\varepsilon_{WSOM/PM0.95}\times\kappa_{WSOM})/\kappa_{PM0.95}\times100$
65	-	-	4±8	4±8
70	-	-	7±7	7±7
75	-	-	10±7	10±7
80	-	-	10±7	10±7
85	13±7	13±7	12±7	12±7

削除：15
削除：08
削除：09
削除：19
削除：11
削除：29
削除：54
削除：04
削除：19
削除：50
削除：48
削除：15
削除：S5

References

Chen, Q., Ikemori, F., Nakamura, Y., Vodicka, P., Kawamura, K., and Mochida, M.: Structural and light-absorption characteristics of complex water-insoluble organic mixtures in urban submicrometer aerosols, Environmental Science & Technology, 51, 8293-8303, 10.1021/acs.est.7b01630, 2017.

Han, Y. M., Kawamura, K., Chen, Q. C., and Mochida, M.: Formation of high-molecular-weight compounds via the heterogeneous reactions of gaseous C-8-C-10 n-aldehydes in the presence of atmospheric aerosol components, Atmospheric Environment, 126, 290-297, 10.1016/j.atmosenv.2015.11.050, 2016.

Jung, J. S., Kim, Y. J., Aggarwal, S. G., and Kawamura, K.: Hygroscopic property of water-soluble organic-enriched aerosols in Ulaanbaatar, Mongolia during the cold winter of 2007, Atmospheric Environment, 45, 2722-2729, 10.1016/j.atmosenv.2011.02.055, 2011.

Park, K., Kittelson, D. B., Zachariah, M. R., and McMurry, P. H.: Measurement of inherent material density of nanoparticle agglomerates, J. Nanopart. Res., 6, 267-272, 10.1023/B:NANO.0000034657.71309.e6, 2004.

Petters, M. D., and Kreidenweis, S. M.: A single parameter representation of hygroscopic growth and cloud condensation nucleus activity, Atmospheric Chemistry and Physics, 7, 1961-1971, 10.5194/acp-7-1961-2007, 2007.

Tang, I. N., and Munkelwitz, H. R.: Water Activities, Densities, and Refractive-Indexes of Aqueous Sulfates and Sodium-Nitrate Droplets of Atmospheric Importance, Journal of Geophysical Research-Atmospheres, 99, 18801-18808, 10.1029/94jd01345, 1994.